Aus der
Klinik und Poliklinik fuer kleine Haustiere
des Fachbereiches Veterinaermedizin
-Freie Universitaet Berlin-

Cardiologic examinations in ferrets with and without heart disease

Inaugural-Dissertation
zur Erlangung des Grades eines
Doktors der Veterinaermedizin
an der
Freien Universitaet Berlin

vorgelegt von
Chavalit Boonyapakorn
Tierarzt aus Pathum Thani, Thailand

Berlin 2007
Journal Nr. 3166

Gedruckt mit Genehmigung des Fachbereichs Veterinaermedizin der Freien Universitaet Berlin

Dekan:	Univ.-Prof.Dr. Leo Brunnberg
Erster Gutachter:	Univ.-Prof.Dr. Eberhard Trautvetter
Zweiter Gutacter:	Prof.Dr. Heike Toenhardt
Dritter Gutacter:	PD Dr. Marianne Skrodzki

Deskriptoren (nach CAB-Thesaurus): Ferrets, heart diseases, auscultation, radiography, electrocardiography, echocardiography

Tag der Promotion: 19.12.2007

Contents

Abbreviations

A

AMV	anterior mitral valve cusp
AO/AOV	aortic valve
AV block	atrioventricular block
AV valve	atrioventricular valve
AV bundle	atrioventricular bundle
AV node	atrioventricular node

B

bpm	beat per minute
BUN	blood urea nitrogen

C

C	cervical vertebra
CaVC	caudal vena cava
Cd	coccygeal vertebra
CF Doppler	color flow Doppler
CH	chordae tendinae
CHF	chronic heart failure
cm	centimeter

D

2-D	two dimensional mode
DCM(P)	dilated cardiomyopathy
DV	dorsoventral

E

ECG	electrocardiogram
e.g.	exempli gratia
EPSS	E point to septal separation

F

Fig	figure
FS	fractional shortening

G- K

g	gram
HR	heart rate
ICS	intercostal space
IVS	interventricular septum
IVSd	interventricular septum at diastole
IVSs	interventricular septum at systole
kg	kilogram

L

L	long axis
LA	left atrium
LA/AO	left atrium/aorta ratio
Lat	lateral
Lat L	lateral long axis
Lat S	lateral short axis
Lat T5-8	T5-8 length on the lateral view
LBBB	left bundle branch block
LC	left coronary cusp of aortic valve
LL	left lateral
LPA	left pulmonary artery
LV	left ventricle
LVd/ LVDd	left ventricular dimension at diastole
LVET	left ventricular ejection time
LVID	left ventricular internal diameter
LVOT	left ventricular outflow tract
LVs/LVDs	left ventricular dimension at systole
LVW	left ventricular wall
LVWd	left ventricular wall at diastole
LVWs	left ventricular wall at systole

M

Max	maximum
m/sec	meter per second
MEA	mean electrical axis
Min	minimum
min	minute
mm	millimeter
mm/sec	millimeter per second
M-mode	motion mode
MV	mitral valve
mV	millivolt

N

NA	not avaliable
NC	noncoronary cusps of aortic valve
NSD group	non sedated-disease group
NSN group	non sedated-normal group

P

PA	pulmonary artery
PE	pericardial effusion
PEP	pre ejection period
PM	papillary muscle
PMI	point of maximal intensity
PMV	posterior mitral valve cusp
PPM	posterior papillary muscle
PV	pulmonary vein
PVR	physiologic valve regurgitation

R	
RII	R wave in lead II
RA	right atrium
Rau	right auricle
RBBB	right bundle branch block
RC	right coronary cusp of aortic valve
RPA	right pulmonary artery
RV	right ventricle
RVO/RVOT	right ventricular outflow tract
RVW	right ventricular wall
S	
S	short axis
S1	first heart sound
S2	second heart sound
S3	third heart sound
S4	fourth heart sound
SA	sinoatrial node
SD	standard deviation
SD group	sedated-disease group
sec	second
SN group	sedated-normal group
SR	sinus rhythm
SVT	supraventricular tachycardia
T	
T	thoracic vertebra
TV	tricuspid valve
V	
V	vertebra
V.c.c	caudal vena cava
VD	ventrodorsal
VHS	vertebral heart sum or vertebral heart size or vertebral heart score
VHS Lat	vertebral heart sum on the lateral view
VPC(s)	ventricular premature complex(es)
VT	ventricular tachycardia
W	
WPW	Wolff-Parkinson-White Syndrome
%	percent
µ	micrometer

1. Introduction

Ferrets or domestic ferrets (Mustela putorius furo) belong to the order of Carnivora, and the family of Mustelidae that includes about 23 genera (Rosenthal, 1994; Fox, 1998A). The genus Mustela was divided into five subgenera: Mustela (weasels), Lutreola (European mink), Vison (American mink), Putorius (ferrets), and Grammogale (South American weasels).

Mustelids have retained many primitive characteristics that include relatively small size, short stocky legs, and five toes per foot, elongated brain case, and a short rostrum. The domestic ferret, Mustela putorius furo, has a long body, with short muscular legs and a long tail. The adult's average body length of 44 to 46 centimeter (cm) from the nose to the tip of the tail was reported by Fox (1998A) and the average body length (without the tail) at 30 - 40 cm. The eyes are small and the ears are short. The neck is cylindrical and noticeably long and blends gradually with the cylindric and elongated thorax and abdomen (Evan and An, 1998). The body weight of intact male ferrets ranges from 1.0- 2.0 kilogram (kg) and 0.5-1.0 kg in intact females (Brown, 1997). Besch-Williford (1987) reported the ferret body weight in male and female were 1.0-2.7 kg and 0.45-0.9 kg respectively. The average life span of the ferret was 5-11 year (Fox, 1998B). Brown (1997) reported that the average life span of the ferret in the United States was 5-8 years and some ferrets may reach 12 years of age. The sexual maturity is reached at 4-8 month of age in one report and 6-12 month of age in the other (Brown, 1997; Fox and Bell, 1998). The female ferret has a gestation period of 42+/- 2 days, the litter size averages 8 kits (range 1-18 kits) and the normal weight at birth is 6-12 gram (g) (Fox, 1998) and 5-15 g (Isenbuegel and Frank, 1985). The kits are weaned for 6-8 weeks of age (Brown, 1997; Fox and Bell, 1998).

Ferret (Mustela putorius furo) has been domesticated for over 2000 years (Oxenham, 1991; Rosenthal, 1994; Ivey and Morrisey, 1999). Initially domestic ferrets were used as hunting animals for control of wild or native rabbits and rodents (Rosenthal, 1994; Brown, 1997). In the United States, the domestic ferrets are primarily maintained as a pet for approximately 300 years (Brown, 1997). It is estimated that there are eight millions ferrets kept as pets, making them the third most popular mammalian pet in the United States (Gehrke, 1997). In more recent years, the ferrets have been used in biomedical research and cardiovascular studies have increased dramatically (Fox, 1998A). Therefore more clinical cardiovascular data are required to examine and treat ferrets with heart-lung disease adequately.

2. Review of literature

2.1 Cardiovascular anatomy

2.1.1 Thoracic cavity

The shape of the thoracic cavity is narrow cranially and continues to wide caudally, making it cone shaped. It composes 14-15 pairs of ribs and nine sternal vertebrae (Brown, 1997; Evan and An, 1998). Some ferrets have 14 ribs on one side and 15 on the other. Normally, the first 10 pairs of ribs are attached to the sternum and the last 4-5 pairs of ribs join each other distally becoming the costal arch. The first pair of ribs is quite short, resulting in a narrow thoracic inlet. The thoracic cage formed by the thoracic walls laterally and the dome-shaped diaphragm caudally. The thoracic inlet is bounded dorsally by the longus coli muscles, and ventrally by the fused unit of the manubrium and the second sternebra. The thoracic inlet contains the trachea, the esophagus, the cranial mediastinum, vessels, and nerves.

The mediastinum is part of the extrapleural space within the thorax and it divides the thorax into the right and left hemithorax. The mediastinum is divided into three parts, the cranial, middle and caudal portion (Evan and An, 1998). The cranial mediastinal cavity is located in front of the heart; the middle mediastinal cavity contains the heart; and the caudal mediastinum lies behind the heart. The pleurae are serous membranes covering the walls of the thoracic cavity, the lungs and the mediastinum. The pleurae form the left and right pleural sacs composing the pleural cavities.

2.1.2 The lungs and associated structures (Figure 1)

The lung of the ferret is formed by six lobes, extending from the first and second to the tenth and eleventh intercostal space (ICS) in an embalmed animal. The left lung consists of the left cranial and left caudal lobe whereas the right lung contains of four lobes, the right cranial, the right middle, the right caudal and the accessory lobe. The ventral border of the right cranial lobe is concave and in conjunction with the middle lobe, it forms a cardiac notch. The trachea is composed of C-shape hyaline cartilages. It is about 9.0 cm long and 0.5 cm in diameter and bifurcated into a left and right main bronchus at the level of the fifth ICS. Each main bronchus is subdivided into a cranial, middle and caudal portion (Evan and An, 1998).

2.1.3 The heart and associated structures (Figure 1)

Heart: The heart is divided into four chambers by cardiac valves and septa. The heart is located more caudally within the thorax than in dogs and cats; it extends from the sixth to eighth rib and has a smaller right ventricle (RV) than most animals in relation to the left ventricle (LV) (Smith and Bishop, 1985; Bixler and Ellis, 2004). The heart is covered largely

by the lung. The cardiac notch is greatest on the right side and extends between the sixth to the tenth rib, which allows a small region of the pericardium to contact the lateral chest wall.
The apex of the heart is directed ventrocaudally and separated from the diaphragm by a distance of approximately ten millimeters (mm) (Truex et al., 1974; Andrews et al., 1979). The phrenicopericardial ligament that connects the heart to the sternum (Budras et al., 2000) may contain a varying amount of fat. Truex et al. (1974) reported that the mean heart weight of twelve male ferrets with a mean body weight of 1102 g was 5.0 g (0.45 percent (%) of total body weight) and the mean heart weight in ten females with a mean body weight 780.8 g was 3.7 g (0.47% of total body weight). The longitudinal axis of the heart formes an angle of approximately 73 degrees with the vertical plane. Dorsoventrally, the heart axis formed an angle of approximately 26 degree with the median plane (Evans and An, 1998).
The heart is covered by the pericardium, a thin, strong fibrous sac which is lined out by a serous membrane. The pericardial sac contains little serous fluid that gives a lubricated surface for the heart (Detweiler, 1984A). The heart is consisting of three layers, the endocardium: the inner layer of the chambers, the myocardium: the cardiac muscle, and the epicardium covering the myocardium.
In small animals, the left and right atria are relatively thin walled structures. There are four openings into the right atrium (RA): (1) the cranial vena cava: the cranial vena cava has a diameter of 3.0 to 3.5 mm (and drains the blood from the head, neck, thoracic limbs, and adjacent abdominal wall; the azygos vein drains the intercostal veins into the right atrium by entering the cranial vena cava; (2) the caudal vena cava returns the blood from the pelvic limbs, abdominal viscera and part of the abdominal wall; (3) the coronary sinus enters the right atrium from the left and is located below the opening of the cranial vena cava; (4) the right atrioventricular orifice is surrounded by the tricuspid valve (TV) (Fox et al., 1999).
The right ventricle is cranioventral to the left ventricle. It receives blood from the right atrium through the tricuspid valve and pumps it out through the pulmonary artery (PA). The left ventricle is presenting the majority of cardiac mass, characterized by a relative thick myocardial wall compared to the other parts of the heart. The left ventricle is filled with blood across the mitral valve (MV) and pumped out of the heart through left ventricular outflow tract (LVOT) across the aortic valves (AO) and aorta. The papillary muscles are conical, slender muscular projections from the ventricular wall attached to the chordae tendineae. Within the right and left ventricle, the multiple papillary muscles are located (Morgan and Travers, 1998). Chordae tendineae are fibromuscular strands usually arising from the apex of a papillary muscle and anchored to the free margin of the atrioventricular valve cusps.

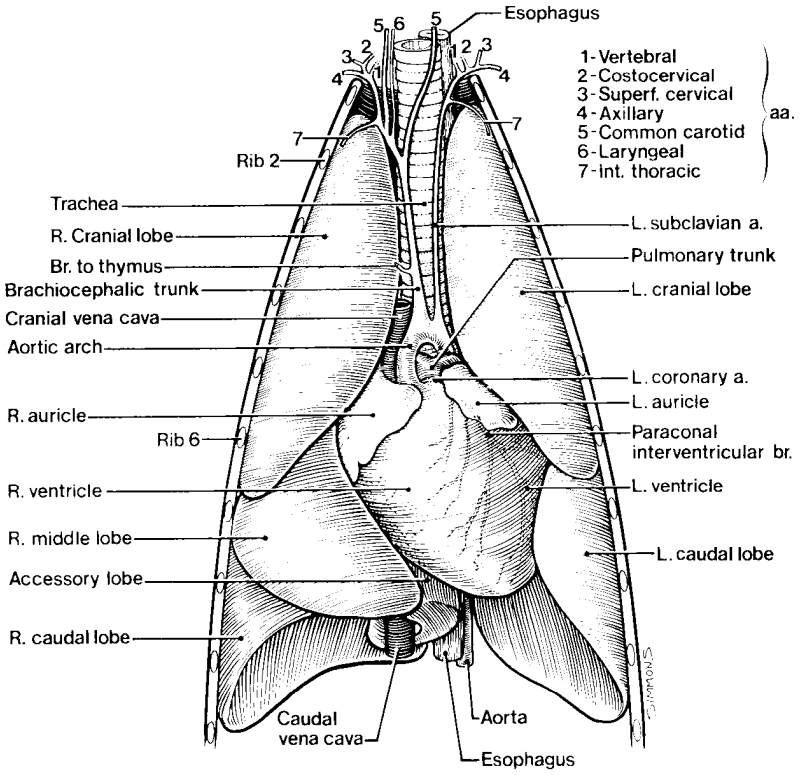

Figure 1: Ferret heart and lung in situ demonstrated from the ventral view. (Evans and An, 1998)

In the mammalian heart, the cardiac valves originate from the annulus fibrosus, a skeleton fibrous ring that surrounds the orifice of aorta, pulmonary artery and atrioventricular valves (AV) (Figure 2). These rings are providing attachment sites for the cardiac valves and for the origin and insertion of the cardiac muscles (Detweiler, 1984A). During diastole, the aortic and pulmonic valves close first to prevent regurgitation back into the ventricles. Then, the AV valves open as blood travels from the atria to fill the ventricles. During the ventricular systole, aortic and pulmonic valves are opened by ejecting ventricular blood into the great vessels, while the AV valves are closed.

Great blood vessel: Andrews et al. (1979) reported the distribution of the great vessels of the ferret heart. The arch of the aorta is buried entirely in pericardial fat and does not emerge from the fibrous pericardium. The aortic arch gives rise to two major branches, the central innominate artery and the left subclavian artery. The innominate artery, also called the brachiocephalic trunk, is estimated 1.5-2.0 mm in diameter (Willis and Barrow, 1971). It is running for 25.0-30.0 mm ventral to the trachea. At the level of the thoracic inlet in divides into three branches, the right and left carotid arteries and right subclavian artery, all of equal diameter of 1.0-1.2 mm. The left subclavian artery has 0.5-0.75 mm in diameter and travels along the trachea to the level of the first rib.

The pulmonary trunk carries non-oxygenated venous blood from the right ventricle to the lungs. It arises from the fibrous pulmonary ring and bifurcates at the respective lung into the left and right pulmonary arteries. The right pulmonary artery is longer than the left pulmonary artery and branches into the right cranial, the middle, the caudal and the accessory lobe. The left pulmonary artery branches into the cranial and caudal lobe. The pulmonary veins (PV) return oxygenated blood from the lungs into the left atrium. There are at least one-possibly two veins from each side of the lung entering the left atrium (Evan and An, 1998).
The cranial and caudal vena cava are large vessels that return the deoxygenated blood to the heart. Each vena cava is approximately 3.0-3.5 mm in diameter (Andrews et al., 1979).
The coronary artery supplies blood to the myocardium. In the ferret heart the left coronary artery is dominant. The coronary sinus of the right atrium collects all the deoxygenated blood from the myocardial circulation. The coronary sinus and its venous myocardial tributaries correspond to the patterns observed in cats, dogs, monkey and human (Truex et al., 1974).

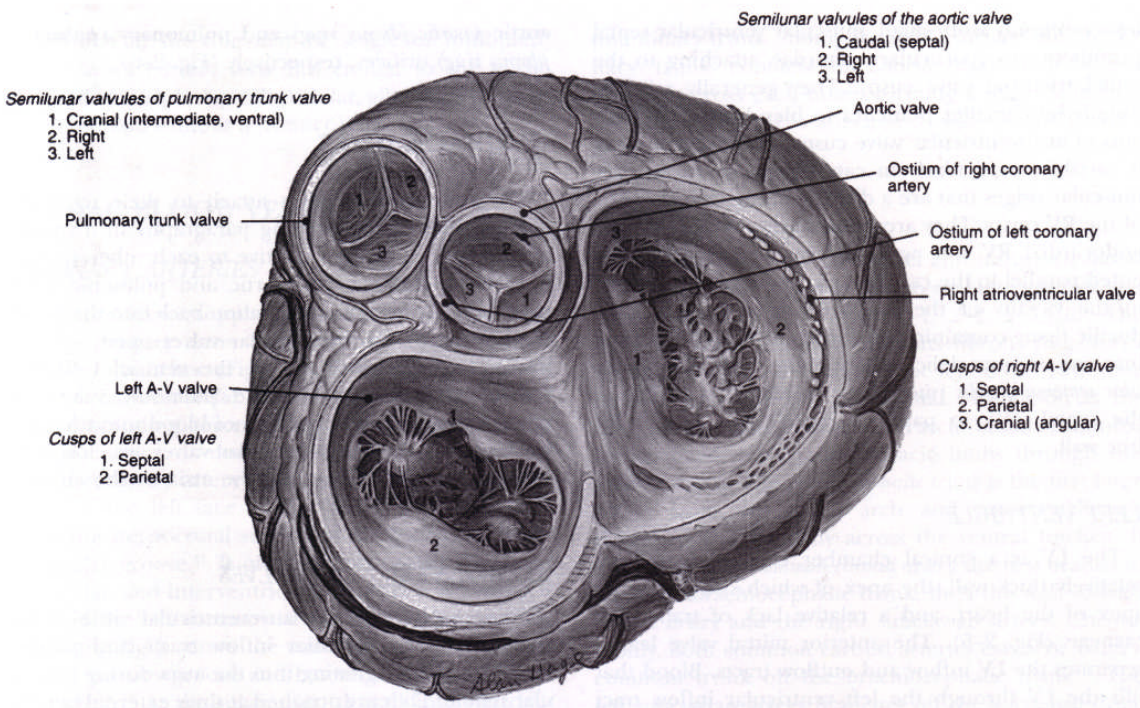

Figure 2: Craniodorsal view of heart base. The annulus fibrosus is forming the fibrous ring that surrounds the orifice of aorta, pulmonary artery and atrioventricular valves and providing the attachment sites for the cardiac valves and for the origin and insertion of the cardiac muscle. (Fox et al., 1999)

2.1.4 Cardiac conduction system (Figure 3)

The heart conduction system is consisting of the sinoatrial node (SA node), the atrioventricular node (AV node) and the atrioventricular bundle of His. Truex et al. (1974) reported that the SA node was a pearly-gray mass of pacemaker cells. A microscopic study showed that the SA node is a 3.0 mm in length, 1.5 mm in width and 1.0 mm thick. It is a compact network of lightly staining cells with a mean cytoplasmic diameter of 6.7 micrometer (μ). Along the epicardial surface of the SA node lie numerous ganglion cells, nerve bundles, and strands of fine beaded autonomic nerve fibers penetrating into the depths of the entire SA node. Most of the SA node receives the blood form the left coronary artery. In some animals it is supplied by the right coronary artery (Truex et al., 1974).

AV node and atrioventricular bundle (AV bundle) are pearly-gray structures that contrast to the more brownish color of the atrial myocardial cells. Fine strands of AV bundle cells have a segment above the annulus fibrosus, before it penetrates the annulus fibrosus, trigone and then reassemble into a compact 1.0 mm bundle at the top of the muscular interventricular septum (IVS) (Marino, 1979). The AV bundle cells vary in total length from 2.0-3.0 mm. The left and right bundle branches were found in the subendocardium on the left and right side of the IVS. Purkinje cells of the bundle branches are the largest cells of the conduction system in the ferret. The mean cytoplasmic diameter of the Purkinje cells in the left and right bundle branch is 10.1 μ and 9.9 μ respectively (Truex et al., 1974).

2.1.5 Cardiac nerves

In all mammals the general anatomic plan of the cardiac nerves are similar but differ in detail in various species (Detweiler, 1984C). The cardiac nerves arise bilaterally from the parasympathetic (vagal) trunk and the sympathetic trunk. Andrews et al. (1979) reported that the vagus nerve and sympathetic trunk lie close and bound together in the same fascial sheath in the neck. The vagosympathetic trunk travels in close proximity to the common carotid artery, lying slightly dorsolateral to it. On the right side, the right vagus nerve is separated from the sympathetic trunk and the middle cervical ganglion at the level of the thoracic inlet and continues caudally to the thoracic cavity. At the level of the fourth thoracic vertebra (T4) to the sixth thoracic vertebra (T6), the vagus sends several small branches that travel on the ventral surface of the trachea. These small vagal branches might be joined by small branches given off by the sympathetic trunk. The combined sympathetic-vagal branches travel on the ventral surface of the trachea until they reach the heart. On the left side, the left sympathetic trunk separates from the vagus in a similar pattern to that of the right. At the point of T4, the left vagus gives off a left recurrent laryngeal nerve which travels with the vagus to the arch of the aorta. Just below the point at which the left recurrent laryngeal nerve is given off, the left vagus gives off a major branch which travels to the aorta

where it forms a fine plexus under the arch of the aorta. The left vagus also sends 2-3 branches to join the branches given off by the right vagus traveling also to the right atrium (Andrew et al., 1979).

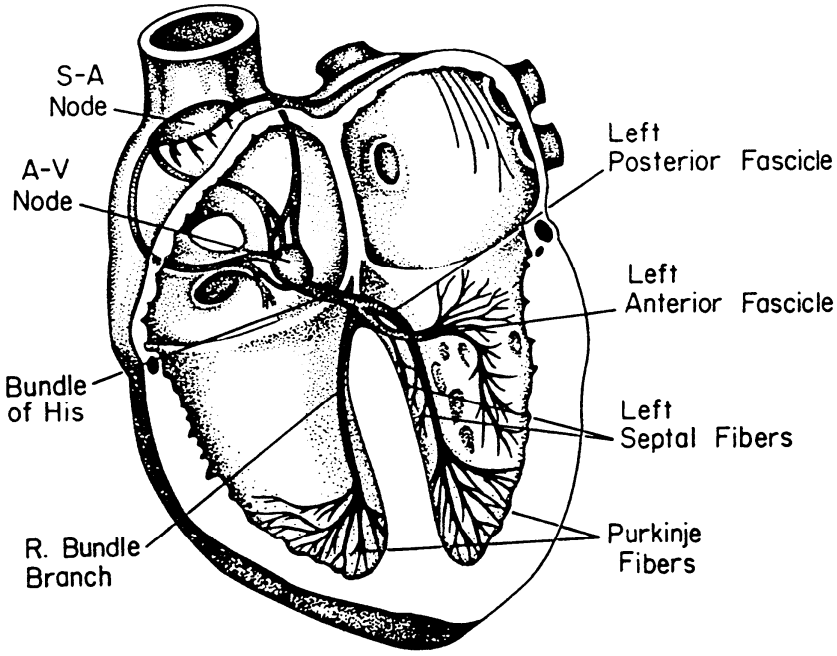

Figure 3: The heart conduction system composes of the sinoatrial node (SA node), the atrioventricular node (AV node), the bundle of His and the left and right bundle branch (Tilley, 1985).

The sympathetic nerves have positive and the vagal fibers have negative chronotropic and inotropic action on the heart. Vagal stimulation slows the discharge rate of the SA node, slow or block AV conduction, it decreases atrial and to a small extent ventricular contractility. Parasympathetic tone is influenced by respiratory activity, ocular pressure, intracardiac and intrapulmonary receptors and stimulation of the carotid sinus. Variation in parasympathetic tone, sinus arrhythmia, is mediated through the vagus nerve. It causes cardiac rate and rhythm to change (Edwards, 1987). Sinus arrhythmia is the normal physiological arrhythmia in dogs and may occur in calm laboratory ferrets but is not usually seen in cats unless some disease state exists. Sympathetic stimulation has the opposite effect and its positive inotropic action on the ventricle and atria is powerful.

2.2 Cardiovascular examination techniques

2.2.1 Auscultation

Heart sounds detected during cardiac auscultation play the most valuable role during physical examination for suspected cardiac disease (Kittleson, 1998A). The auscultation should be performed systematically as part of a cardiovascular examination. It usually begins by placing the stethoscope over the point of maximal intensity (PMI) of the mitral valve (Sisson and Ettinger, 1999). PMI refers to the location where the heart sound is loudest. The left chest wall is typically divided with respect to PMI into left heart base that include both aortic and pulmonic area and left heart apex with respect to the mitral valve area. On the other hand, the right chest wall is typically respected to PMI for the tricuspid area (Figure 4). Heart sounds are produced by the certain vibration associated with the pulsatile events of the cardiac cycle (Detweiler, 1984B). Cardiovascular sounds are divided into two groups based on their duration: (1) transients, sounds of relatively short duration and (2) murmurs, groups of sound vibrations of longer duration (Detweiler and Patterson, 1967; Detweiler, 1984B; Sisson and Ettinger, 1999). Transient heart sounds include the two normal heart sounds, first heart sound (S1) and second heart sound (S2), systolic ejection sounds, accentuated third heart sound (S3) and fourth heart sound (S4), and certain abnormal sounds (e.g. clicks and gallop sounds or rhythms). The four normal heart sounds coincide with the following events (Figure 5). The S1 occurs at the onset of the systole. This coincides of the QRS complex on the electrocardiogram (ECG). The S1 is produced by blood turbulence caused by closure of the AV valves and vibrations in the great arteries and is loudest over the mitral area (Gompf, 1988). The hemodynamic events are associated with the closure of the AV valves (mitral and tricuspid), isovolumetric contraction, semilunar valve opening, early ejection (acceleration) of blood into the aorta and pulmonary artery (Detweiler, 1984B). The S2 occurs at the end of ventricular ejection (at the end of systole), after the T wave on the ECG (Kittleson, 1998A). It is produced by blood turbulence during closure of semilunar valves and vibrations of the heart and great vessels (Gompf, 1988). The presence of the S3 and S4 is a pathologic finding and constitutes a gallop rhythm (Gompf, 1988). The S3 occurs at the peak of rapid ventricular filling or shortly after that. It coincides with the initial maximal opening of the mitral valve on the echocardiogram (Kittleson, 1998A). S3 is generated by termination of rapid diastolic ventricular filling especially with ventricular dilatation (e.g. dilated cardiomyopathy, DCMP) or chronic volume overload (e.g. acquired mitral insufficiency) (Gompf, 1988). The S4 is a low-frequency sound generated during atrial systole (late ventricular diastole, Kittleson, 1998A).

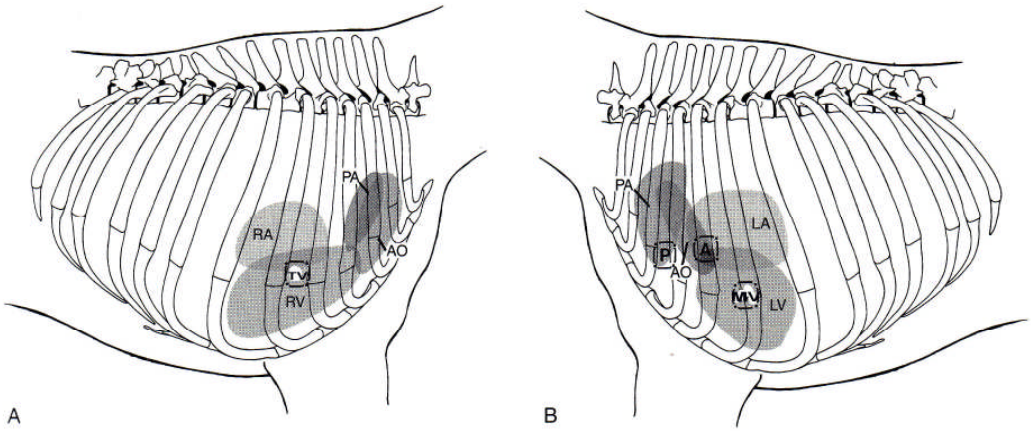

Figure 4: Area for cardiac auscultation in the canine species. (A) Tricuspid valve area (*TV*) located on the right hemithorax. (B) On the left hemithorax the regions for mitral valve (*MV*), aortic valve (*A*), and pulmonic valve area (*P*) are shown. (Fox et al., 1999)

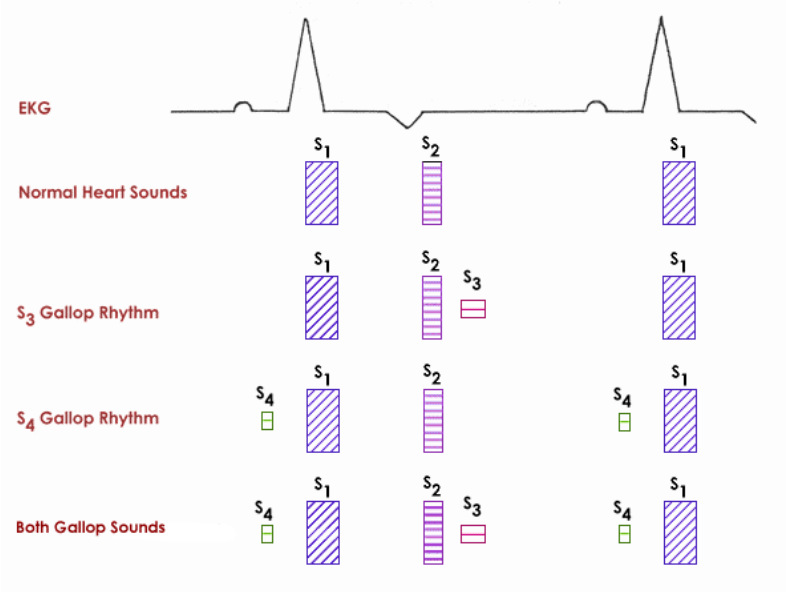

Figure 5: Diagram demonstrating the four normal heart sounds. The S1 occurrs at the onset of the systole. This coincides with the QRS complex in the ECG. The S2 occurrs at the end of ventricular ejection (at the end of systole), after the T wave on the ECG. S3 is generated by termination of rapid diastolic ventricular filling especially with ventricular dilatation. The S4 is a low-frequency sound generated during atrial systole (late ventricular diastole). (www.vetgo.com.)

Murmurs are caused by turbulent blood flow which develops when flow velocity increases, blood viscosity decreases (e.g. anemia), or flow patterns are disrupted (Gompf, 1988). It is arising from the heart or great vessels and possesses a variety of distinguishing characteristics: intensity, timing, radiation, frequency, character and location (Sisson and Ettinger, 1999). Murmurs are divided into (1) functional murmurs (normal heart) and (2) pathologic murmurs (heart disease). Functional murmurs can be caused by anemia, which reduces blood viscosity and increases flow velocity, causing turbulence to increase. Fever

and hyperthyroidism increases the rate of blood flow, which causes also murmurs. Innocent murmurs are present in the newborn animal and disappear by about 4-8 month of age in dogs and cats (Gompf, 1988). Pathologic murmurs are caused by congenital or acquired defects in the heart or great vessels and are often associated with abnormal conditions such as valvular stenosis or insufficiency (Detweiler, 1984B; Gompf, 1988). The intensity or loudness of the murmur can be classified into five grades (Detweiler and Patterson, 1967).

Grade I: The softest audible murmur.

Grade II: A faint murmur, clearly heard after a few seconds auscultation.

Grade III: Immediately heard when auscultation begins and audible over a fairly large area.

Grade IV: The loudest murmur which is still inaudible when the stethoscope chest piece is just removed from the thoracic wall.

Grade V: A murmur remains audible when the stethoscope chest piece is just removed from the thoracic wall.

Intensity of the murmur may also be classified into six grades (Kittleson, 1998A; Sisson and Ettinger, 1999; Gompf, 2001; Kvart and Haeggstroem, 2002; Martin and Corcoran, 2006). A grade 1/6 murmur is the faintest murmur that can be detected and is heard only with particular effort. A grade 2/6 murmur is a faint murmur clearly heard after a few seconds auscultation by an experienced examiner. A grade 3/6 murmur is moderately loud and easily heard. A grade 4/6 murmur is a loud murmur that does not produce a palpable thrill. A grade 5/6 murmur is a very loud murmur that produces a thrill but is inaudible when the stethoscope is removed from the chest wall. A grade 6/6 murmur is a very loud murmur that produces a thrill still audible after the stethoscope is removed from the chest.

2.2.2 Thoracic radiography

Thoracic radiography is one of the most important diagnostic tests used in small animal cardiovascular medicine (Kittleson, 1998B). It is a diagnostic tool to determine the cardiac size, cardiac chambers, vessels and lung parenchyma. The interpretation of normal radiographs in ferrets is adapted from the technique used in dogs and cats (Rosenthal, 2001). The thoracic shape of the ferret is different from the other carnivores. The thoracic cavity of the ferret is quite uniform but elongated and flattened dorsoventrally compared to the other species (Stepien et al., 1999). Evans and An (1998) described the normal ferret heart as cone shaped and placed obliquely in the thoracic cavity. The heart lies approximately between the 6^{th} and 8^{th} rib (Smith and Bishop, 1985). On the ventrodorsal view of the chest, the heart apex is directed to the left of the mid line (Brown, 1997). Occasionally, the heart on the lateral radiograph appears sometimes elevated above the sternum. This is a normal finding in normal ferret radiographs (Rosenthal, 2001).

Normal cardiac measurement:

In small animals, normally, the cardiac silhouette on the lateral view, is measured at the maximum width (at the level of the ventral aspect of the insertion of the caudal vena cava) and perpendicular to the axis from base to apex, is approximately 2.5 ICS in deep-chested breeds and 3.5 ICS in barrel-chested breeds (Buchanan, 1991; Kittleson, 1998B; Sleeper and Buchanan, 2001). On the vertical plane of the lateral view, the distance from the cardiac apex to the carina is normally 2/3 to 3/4 of the vertical distance from the cardiac apex to the vertical column. On the DV view, the greatest cardiac dimension should be less than 2/3 of the chest wall to chest wall thoracic dimension at that location.

In cats, the heart is more elongated and elliptical in shape than in dogs on the lateral view. The ventricular area occupies about 2 to 2½ ICS in the lateral view and it tends to be more horizontal; with cats age, the heart tends to horizontalize even more in geriatric cats (called lazy heart, Kittelson, 1998B).

Recently, a more objective heart size, vertebral scale system, has been formulated by Buchanan and Bucheler (1995). The vertebral scale system has been developed in which cardiac dimensions are scaled against the length of specific thoracic vertebrae. In lateral view, the long axis of the heart (L) is measured with a caliper extending from the bottom of the left mainstem bronchus to the apex of the heart. The caliper is repositioned along the vertebral column, starting at the cranial edge of the fourth thoracic vertebra. The length of the heart is recorded as the number of vertebrae and estimated to the nearest 1/10 of a vertebra. The maximum perpendicular short axis (S) is measured perpendicular to the long axis and recorded in the same manner beginning at the fourth thoracic vertebra. If obvious left atrial enlargement is present, the short axis measurement is made at the dorsal juncture of the left atrial and caudal vena cava silhouettes (Figure 6). The sum of the long and short axis, the vertebral heart sum or vertebral heart size (VHS), was determined to be between 8.5-10.6 vertebra (v) (9.7+/- 0.5v) in dogs (Buchanan and Bucheler, 1995). The dorsoventral (DV) projection is preferred over ventrodorsal (VD) to reduce VD magnification effects and provided more consistency in cardiac contours. DV cardiac measurement in dogs does not add significantly to the information obtained in lateral radiographs (Buchanan, 1991). The same technique was modified for the ferret's heart measurement. The length and width of the cardiac silhouette was compared to the T5-8 thoracic vertebra and estimated to the nearest 0.25 v. On the right lateral view, the measurement from this modified VHS method revealed 5.23-5.47 v (median 5.33 v) from twenty normal adult ferrets (Stepien et al., 1999).

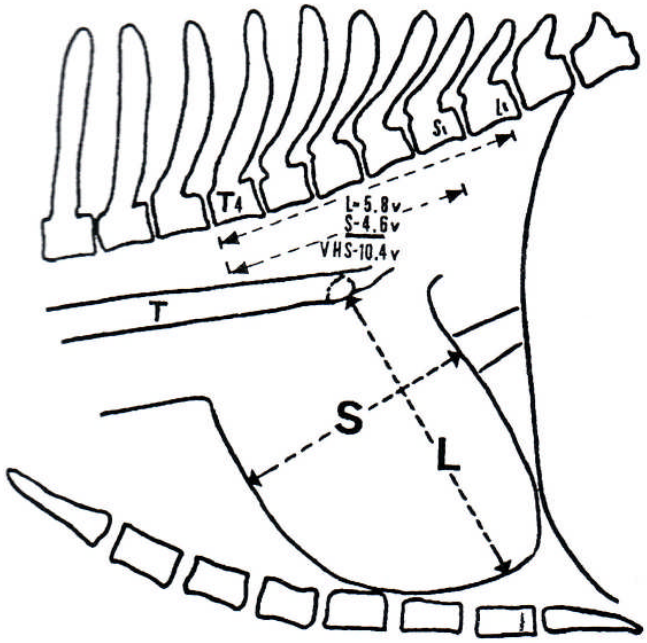

Figure 6: Diagram illustrating the vertebral heart size measurement method. The long axis of the heart (L) is measured from the bottom of the left mainstem bronchus to the apex of the heart. The short axis is measured perpendicular to the long axis. The length of the long and short axis of the heart is recorded as the number of a vertebra beginning at the 4th thoracic vertebra and estimated to the nearest 1/10 of a vertebra. (Buchanan and Bucheler, 1995)

Interpretation of cardiomegaly and main vessels enlargement:

(Kittleson, 1998B; Kealy, 1999; Schelling, 2001; Gavahan, 2003) (Figure 7)

Right atrial enlargement: Right atrial enlargement is often difficult to recognize unless it is severe. On the lateral view it appears as a loss of the cranial waist, bulge in the craniodorsal portion of the cardiac silhouette and the enlarged chamber may displace the trachea that lies cranial to the carina dorsally. On the DV view, right auricle dilation can cause a bulge in the cardiac silhouette from 9 to 11 o'clock.

Right ventricular enlargement: On the lateral view, right ventricular enlargement may increase the contact of the heart to the sternum. On the DV view, it increases the size of cardiac silhouette on the right size of the chest and increases convexity from the 5-6 o'clock position, through to the 10 o'clock position. It may produce the so called reverse D sign because of the right ventricular enlargement.

Left atrial enlargement: Left atrial enlargement in generally is easy to detect in small animals. On the lateral view, the enlarged atrium elevates the distal end of the trachea and the left main stem bronchus with varying degree depending on the severity of the left atrial enlargement. On the DV view, moderate to severe enlargement shows the left auricle bulges at the 2-3 o'clock position.

Left ventricular enlargement: On the lateral view, the entire caudal heart border changes from convex to straight with the combined left atrial and ventricular dilation. On the DV view, the left cardiac border becomes more convex and is approaching the lateral chest wall.

Main pulmonary artery enlargement: Main pulmonary artery enlargement unless severe is generally not identified on a lateral view. On the DV view, it is identified as a bulge at the 1 o'clock to 2 o'clock position.

Aortic enlargement: On the lateral view, ascending aortic enlargement shows the widening of the dorsal aspect of the cardiac silhouette. On the DV view shows the increase extension of the cardiac margin between the 11 and 1 o'clock position.

Interpretation of the lung field:

Interstitial pulmonary edema: The interstitium is an extravascular tissue compartment that expands to accommodate excess transudate fluid, which is drained by the pulmonary lymphatic system. The interstitial pulmonary edema occurs when this process is overwhelmed. On radiography may show as a uniform, poorly defined increase in lung opacity that decreases small vascular sharpness. The walls of the pulmonary vasculature are obscured by edema fluid.

Alveolar pulmonary edema: It is characterized by the absence of pulmonary air contrast. In severe pulmonary edema, the fluid invaded alveolar spaces causing the lung parenchyma to have a similar density to soft tissue. This marked increase in density obscures pulmonary vessels. If the fluids are not flooded into bronchi the air bronchograms, the visualized bronchi as radiolucent within the soft tissue density of the edema-filled lungs, may be observed.

Pleural effusion: Pleural effusion is radiographically evident as focal areas of increased soft tissue opacity located within the thoracic cavity. It causes separation of lung lobes from both the thoracic wall and the adjacent lobes. On lateral radiography it may show an increase in the soft tissue thickness of the caudodorsal thoracophrenic angle and diaphragm as well as an increase of interlobar fissures creating linear densities.

A

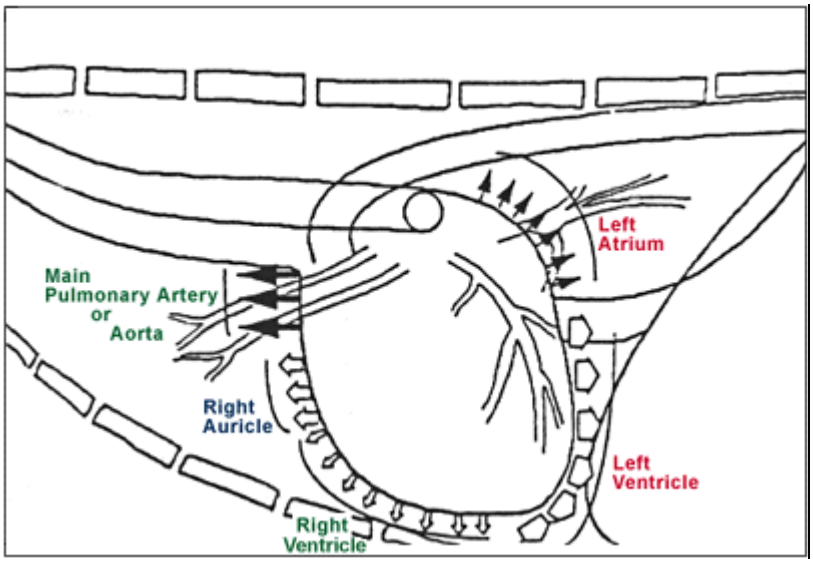

B

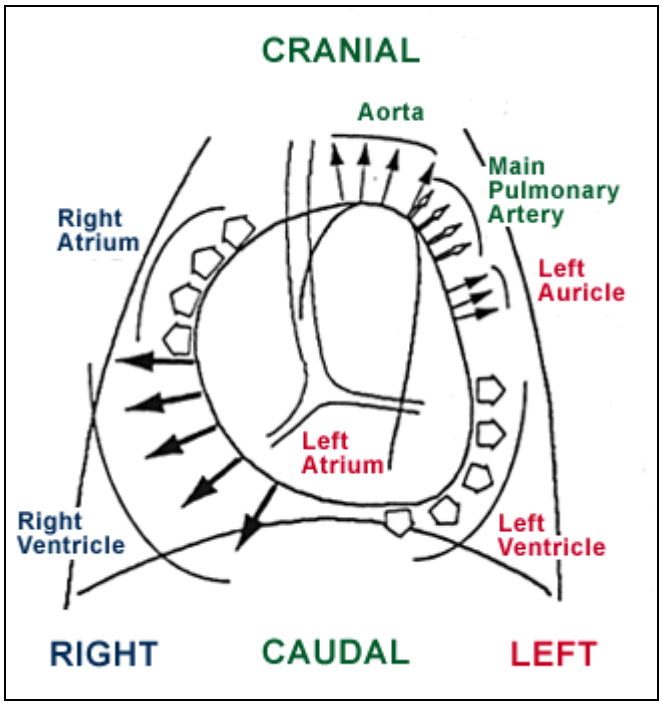

Figure 7: Drawing exhibits the position of cardiac enlargement on the lateral view (A) and DV view (B). In the DV view the enlargement of the RV is also described as reversed D sign. (www.vetgo.com)

2.2.3 Electrocardiography

The normal electrocardiogram

The electrocardiogram (ECG) is measured in amplitude and time of potential differences of the electrical current generated through depolarization and repolarization of cardiac structures (Edwards, 1987). The electrocardiogram was used in clinical practice to diagnose arrhythmias and conduction disturbances and to ascertain myocardial health (Miller et al., 1999). It was also useful in monitoring the status of an animal through many experimental procedures, including those which are not necessarily related to the heart (Smith and Bishop, 1985). The electrocardiogram is a moving record of the deflections generated by the heart and recorded with the stylus of the electrocardiograph calibrated in voltage (vertical axis) and time (horizontal axis). Electrocardiographic electrodes (leads) register cardiac potentials from the body surface. These are measured by the electrocardiograph (galvanometer) and recorded on the standardized graph paper inscribed with 1 mm spaced horizontal and vertical lines (Miller et al., 1999). At the usual standardization of 1 cm equals 1 millivolt (mV), each small box is equal to 0.1 mV. On the horizontal axis, each small box represents 0.02 second (sec) and 0.04 sec at the speed paper 50 millimeter per second (mm/sec) and 25 mm/sec respectively (Figure 8). In the electrocardiogram, the P wave represents the sum of all the electrical forces produced during the depolarization of both atria. The PR (PQ) segment represents the delay of conduction velocity at the AV node to allow the atria time to discharge their blood into the ventricles before the ventricular contraction begins. The PR interval, which includes the P wave plus the PR segment, is a measurement of the time interval from the beginning of atrial depolarization to the beginning of ventricular depolarization. The Q wave is the first negative or downward deflection in all leads in the electrocardiogram, and it represents septal depolarization. The R wave is the first positive or upward deflection of the QRS complex that is produced by ventricular depolarization. Even though both the left and the right ventricles discharge simultaneously, the electrocardiogram records mainly the left ventricular force. That is because the left ventricular forces are higher of magnitude, and usually cancel out the smaller right ventricular electrical force (Edwards, 1987). The first negative deflection following the R wave is the S wave; it represents the depolarization of the posterior basal region of the left ventricle. The ST segment is measured from the end of S wave to the beginning of T wave. The ventricular repolarization is represented by ST segment and T wave. (Figure 9)

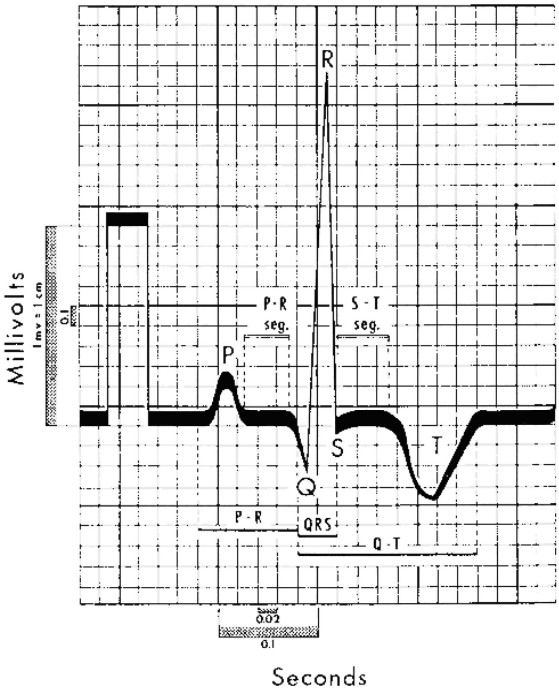

Figure 8: Standard ECG; at the standardization of 1 cm equal to 1 mV, each small box is equal to 0.1 mV. On the horizontal axis, each small box represents 0.02 sec at 50 mm/sec registration. On the electrocardiogram, the P wave represents the sum of all electrical forces produced during the depolarization of both atria. The PR segment represents the delay of conduction velocity at the AV node. The PR interval is a measurement of the time interval from the beginning of atrial depolarization to the beginning of ventricular depolarization. The Q wave represents septal depolarization. The R wave is the first positive or upward deflection of the QRS complex that is produced by the ventricular depolarization. (Bolton, 1975)

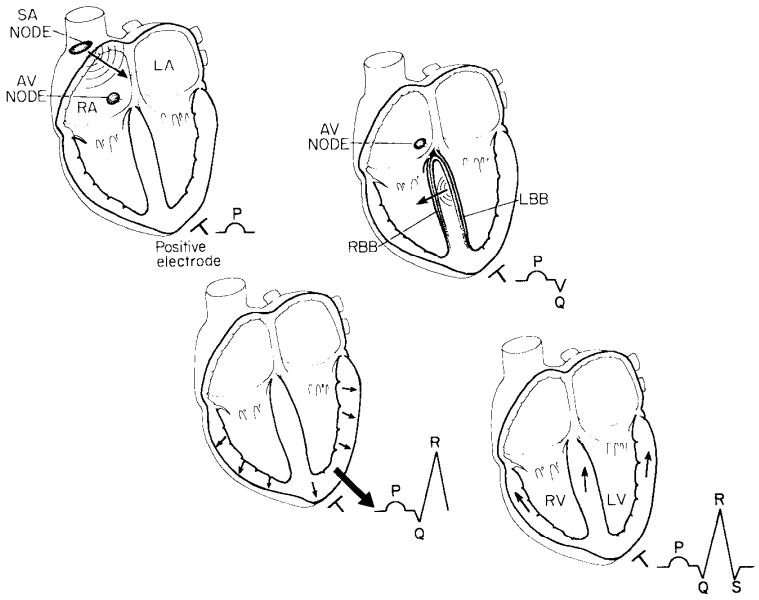

Figure 9: Sequence of electrical impulse conduction and cardiac chamber activations in relation to the electrocardiogram. (Tilley, 1992)

The lead system

The electrocardiographic lead system is composed of bipolar standard limb leads I, II, and III, unipolar limb leads aVR, aVL, and aVF, and unipolar precordial (thoracic) leads CV6LL (V2), CV6LU (V4), CV5RL (rV2) and V10 (Figure 10). The combination of bipolar standard limb leads and augmented unipolar leads produces the basic six-lead system called Bailey's hexaxial lead system which is the most widely used in veterinary electrocardiography. In the six-lead system, the electrodes should be placed just below the olecranon and above the patella for bipolar standard and augmented unipolar limb leads. The standard position for recording an electrocardiogram is the placement of the patient in right lateral recumbency, with the forelimbs and hindlimbs held perpendicular to the long axis of the body and parallel to each other (Edwards, 1987). Alcohol or conducting paste is applied to the skin and electrodes. In lead I, the positive electrode labeled on the left forelimb and the negative electrode on the right forelimb. Lead II has its positive electrode on the left hindlimb and negative electrode on the right forelimb. Lead III also has its positive electrode on the left hindlimb with its negative electrode on the left forelimb.

Chest leads are of limited value in small animals and are rarely used in clinical practice. In small animal practice, it is composed of four common positions, CV5RL, CV6LL, CV6LU and V10. The left chest leads are used mostly to detect right ventricular enlargement and identify P waves that are difficult to see in the other leads. For all other details see table 1.

Table 1: Small animal ECG lead system. (Edwards, 1987)

Bipolar standard limb leads	
Lead I	: right forelimb (-) compared with left forelimb (+)
Lead II	: right forelimb (-) compared with left hindlimb (+)
Lead III	: left forelimb (-) compared with left hindlimb (+)
Augmented unipolar limb leads	
Lead aVR	: right forelimb (+) compared with left forelimb and left hindlimb (-)
Lead aVL	: left forelimb (+) compared with right forelimb and left hindlimb (-)
Lead aVF	: left hindlimb (+) compared with right and left forelimbs (-)
Unipolar precordial chest leads	
Lead CV5RL (rV2)	: fifth right intercostals space near edge of sternum
Lead CV6LL (V2)	: sixth left intercostals space near edge of sternum
Lead CV6LU (V4)	: sixth left intercostals space at costochondral junction
Lead V10	: over dorsal spinous process of seventh thoracic vertebra

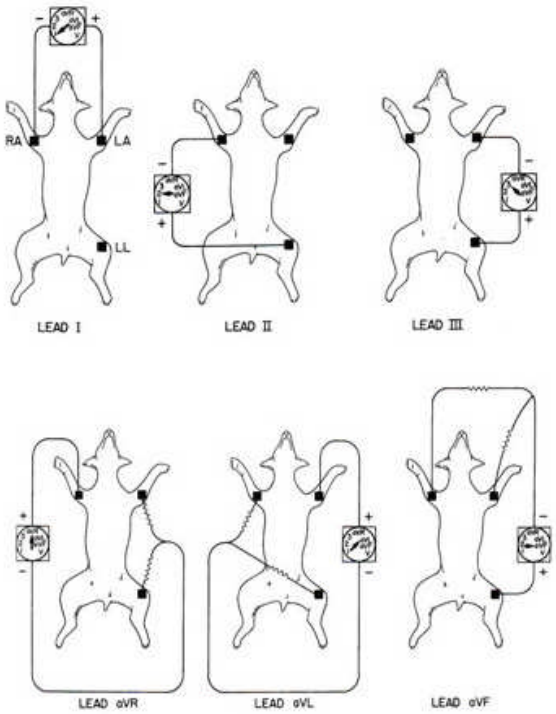

Figure 10: Bipolar standard leads and augmented unipolar limb leads shown in the frontal plane. (Tilley, 1992)

The systematic approach to ECG

The ECGs are interpreted in a systematic manner. Once paper speed, the lead(s) used, and calibration is known, the heart rate, rhythm, frontal axis, and individual wave forms can be determined. Heart rate can be calculated by counting the number of complexes in 3 or 6 sec and then multiplying by 20 or 10, respectively. The alternative method to calculate the heart rate is to count the numbers of small boxes from R wave to R wave and divided into 3000 at the paper speed of 50 mm/sec or 1500 at the paper speed of 25 mm/sec. This method is more accurate and usually used when the rhythm is regular and it is also useful to determine the heart rate in irregular rhythms by checking several RR intervals. The heart rhythm is evaluated by scanning the ECG for irregularities and identifying individual wave forms. The relationship between P wave and the QRS-T complex is also evaluated. The P wave must be present for every QRS complex and all P and all QRS waves should be look alike. Estimation of the mean electrical axis (MEA) is described later.

Ferret ECG wave forms are different from dogs and cats: in lead II, the P waves are small as in cats, whereas the R waves are large as in dogs (Smith and Bishop, 1985; Hoefer, 2001). Smith and Bishop, 1985 reported that all of the ferrets used in one study exhibited a normal sinus rhythm. Other publications reported that the normal ferrets have a pronounced sinus arrhythmia that can be quite dramatic on auscultation (Hillyer and Brown, 1994; Hoefer, 2001A). Bone et al, 1988 studied the electrocardiograms in 25 clinically normal male ferrets anesthetized with ketamine-xylazine and from seven ferrets anesthetized with the ketamine

alone, the results show that the QRS in lead I was positive in 23 ferrets and isoelectric in two ferrets. The QRS in lead II, III, and aVF were positive in all animals. The QRS in augmented limb leads aVR and aVL was negative in all of the ferrets. In precordial lead V10, QRS was negative in 23 ferrets and slightly positive in two ferrets (Bone et al., 1988). Table 2 shows the electrocardiographic values which have been described in clinically normal ferrets sedated by using a ketamine-xylazine combination.

Table 2: Comparative ECG parameters from lead II in three studies. All animals were sedated with ketamine-xylazine combination. Group A: from Fox, 1998, Group B: from Randolph, 1986, Group C: from Bone et al., 1988. NA = not available.

ECG parameter	Group A		Group B		Group C	
	Mean± SD	Range	Mean ± SD	Range	Mean± SD	Range
Heart rate (bpm)	233±22	NA	224 ± 51	150-340	196 ± 26.5	140-240
P amplitude (mV)	0.122 ± 0.007	NA	0.106 ± 0.03	0.05-0.20	NA	NA
P duration (sec)	0.024 ± 0.004	NA	0.03 ± 0.009	0.015-0.04	NA	NA
PR interval (sec)	0.047 ± 0.003	NA	0.05 ± 0.01	0.04-0.08	0.056 ± 0.009	0.04-0.08
Q amplitude (mV)	0.1 ± 0.001	NA	NA	NA	NA	NA
QRS duration (sec)	0.043 ± 0.003	NA	0.049 ±0.008	0.04-0.06	0.044 ± 0.008	0.035-0.06
R amplitude (mV)	1.46 ± 0.84	NA	1.59 ± 0.63	0.6-3.15	2.21 ±0.42	1.4-3.0
S amplitude (mV)	0.125 ± 0.025	NA	0.166 ± 0.101	0.1-0.25	NA	NA
ST segment (sec)	0.036 ± 0.016	NA	0.030 ± 0.016	0.01-0.06	NA	NA
QT interval (sec)	0.12 ± 0.04	NA	0.13 ± 0.027	0.10-0.18	0.109 ± 0.018	0.08-0.14
T duration (sec)	0.05 ± 0.02	NA	0.06 ± 0.01	0.03-0.1	NA	NA
T amplitude (mV)	0.22 ± 0.12	NA	0.24 ± 0.12	0.10-0.45	NA	NA
MEA (frontal plane)	77.22 ± 12	NA	NA	65-100	64.84 ± 20.49	26.6-90

ECG abnormalities
(Bolton, 1975; Trautvetter, 1986; Edwards, 1987; Tilley, 1992; Ware, 1998; Kittelson, 1998C-D; Miller et al., 1999; Tilley and Goodwin, 2001)

Chamber enlargement

Atrial enlargement: The P wave in ECG indicates atrial depolarization. The enlargement of both right and left atrium can be detected by measuring the height and width of the P wave. The term P pulmonale is used to describe the tall and peaked P waves that indicate right atrial enlargement. The P wave becomes wide and notched when the left atrium is enlarged and can be called P mitrale.

Right ventricular enlargement: The enlargement of the right ventricle is usually marked by the time there is evidence in the ECG. The right axis deviation and deep S waves in lead I are a strong criteria for right ventricular enlargement and also right bundle branch block. The other criteria are deep S waves in lead I, II, III, and aVF and QS (W shape) in V10 as well as positive T wave in V10.

Left ventricular dilation and hypertrophy: It can be detected by an increase of the R wave amplitudes in all limb leads. A left axis deviation may be shown when a concentric hypertrophy is accompanied.

Arrhythmia

The cardiac arrhythmia can be classified by using anatomical and physiological terms into (1) sinoatrial arrhythmia (2) ectopic arrhythmia (3) conduction disturbances (table 3). The sinus rhythm is characterized by the occurrence of P waves before each chamber complex and the timing between QRS complexes are regular. Sinus arrhythmia is usually caused by respiratory influences. It is characterized by a cyclic slowing of sinus rate during expiration and speeding of sinus rate during inspiration. The P wave configuration may also change in shape during respiration. Wandering pacemaker is characterized by a taller P wave configuration during inspiration and a flat one in expiration. Sinus arrhythmia is normal in dogs and generally abnormal in cats. It has also been described in ferrets by Grauwiler (1965). Sinus bradycardia and sinus tachycardia are rhythms that originate in the SA node and are conducted normally but the rate is slower than average normal rate in sinus bradycardia and faster than average normal rate in sinus tachycardia. Ectopic arrhythmia is created by the abnormal impulses that originate outside the SA node. Ectopic impulses can be classified into supraventricular and ventricular in origin. Supraventricular premature beats (complexes) (SVP) are the impulses that originate in the atrium (atrial premature beats) or at the AV junction (junctional premature beats). Some veterinary cardiologists have classified atrial premature beats from junctional premature beats by using the P wave configuration. In atrial premature beats, a P wave is altered but positive in deflection; on the other hand, a P wave is abnormal and negative in deflection in junctional premature beats (Bolton, 1975).

Because of no absolute criteria to distinguish an atrial ectopic site from a nodal (junctional) ectopic site (Kittleson, 1998C), it is more important to distinguish whether an arrhythmia originates from above the AV node (supraventricular) or below it (ventricular). Supraventricular premature complexes usually depolarize the sinus node, resetting the sinus rhythm and creating a non compensatory pause. It is characterized by an RR interval enclosing the premature complex that is less than twice the normal RR interval duration.

Atrial tachycardia is characterized by four or more atrial premature complexes in succession. The P wave differs from normal but the QRS complex remains normal in shape (very similar to the sinus impulses). In some case it may be difficult or impossible to differentiate a supraventricular tachycardia (SVT) from a ventricular tachycardia (VT). That may be the case if SVT exists with coexisting bundle branch block. Atrial flutter is caused by very rapid, regular, continuously perpetuated waves of electrical activation throughout the atria. In the ECG, the base line is replaced by sawtooth flutter waves (F waves). It is not a stable rhythm and often degenerates into atrial fibrillation or changes back into normal rhythm. Atrial fibrillation is characterized by rapid, chaotic atrial activation. P waves are absent and the baseline may show irregular undulations (fibrillation wave or f waves). RR intervals are irregular.

Ventricular premature complexes (VPC) are impulses that arise from an ectopic ventricular focus. These abnormal depolarizations spread from cell junction to cell junction and slow the conduction velocity down compared to the normal impulse which spreads through the Purkinje system. This result makes the QRS complex wide and bizarre in contour. P waves are normal in form but not associated with QRS complexes. Generally the VPC can not penetrate the atrium retrogradly through the AV junction, therefore the SA node is not depolarized and can not reset this node as it occurs in supraventricular premature complexes and therefore the sinus rhythm continues undisturbed after the VPC. Thus the VPC is followed by compensatory pause in the sinus rhythm i.e., the interval between the sinus complexes preceding and following the premature complex equals twice the normal conducted RR interval. The VPC can occur single, in pairs, or series. The term ventricular tachycardia is used to define a continuous series of three or more successive VPC. If every other beat is a VPC, it is called ventricular bigeminy. When every third beat is a VPC, it is termed ventricular trigeniny. The term capture beat refers to the successful conduction of a P wave into the ventricle, uninterrupted by another VPC. If the normal QRS complex is combined with a VPC, it is called a fusion complex. The lethal rhythm characterized by chaotic electrical activities of the ventricle is called ventricular fibrillation. Ventricular asystole is a term referred to the absence of ventricular electrical and mechanical activities.

An escape complex is a complex that occurs after a long pause in a dominant rhythm (usually sinus rhythm). If the dominant rhythm is not resumed, the ectopic focus (junctional or ventricular tissue) may discharge at its own intrinsic rate.

AV node conduction disturbances occur as first, second and third (complete) AV block. First degree AV block is characterized by a prolonged PR interval on the ECG tracing. It represents the prolonged conduction impulse of the sinus node to the ventricular conduction system. Second degree AV block is an intermittent failure of AV conduction that can divided into two subtypes, (1) Mobitz type1 (Wenckebach) is characterized by progressive prolongation of the PR interval until a non conducted P wave occurs and the QRS complex is skipped (2) Mobitz type2 there is no progressive PR interval prolongation preceding the blocked P wave. Third degree AV block or complete AV block is a term used to describe the absence of AV conduction. The ventricle is depolarized by pacemakers originating below the block usually from the ventricular myocardium. This ECG is characterized by P waves which do not relate to the QRS complexes.

Sinoatrial standstill is characterized by absence of P waves and a regular escape rhythm with QRS complexes of supraventricular configuration.

Bundle branch block refers to the disruption of impulse transmission through the right or left branches below the bundle of His. Right bundle branch block (RBBB) is a delay or block of conduction in the right bundle branch. It results in right ventricular depolarizing through myocytes by impulses that pass from the left bundle branch to the right side of the septum below the block, instead through the Purkinje network. ECG characteristics of RBBB are (1) right axis deviation (2) the QRS complex is positive in aVR, aVL, and CV5RL and has a wide RSR' or rsR' pattern in CV5RL (3) QRS complexes have large, wide S waves in leads I , II, III, aVF, CV6LL, and CV6LU. Left bundle branch block (LBBB) results from conduction delay or block in the left bundle branch. It causes the impulse to activate the right ventricle first through the right bundle branch. The left ventricle is activated later and more slowly, having an impulse transmission through myocytes instead of Purkinje fibers. This causes the QRS complex to become prolonged in duration which means longer than 0.05 to 0.06 sec. The QRS complex is wide and positive in lead I, II, III and aVF. LBBB must be differentiated from a left ventricular enlargement pattern. Absence of left ventricular enlargement in radiographs and echocardiographs supports the diagnosis of LBBB.

Wolff-Parkinson-White Syndrome (WPW) is a congenital abnormality in which an accessory pathway bypasses the AV node and conducts atrial impulses directly to the ventricle. Three accessory conduction pathways are described for WPW: bundle of Kent (accessory AV connections), James' fibers (AV nodal bypass tracts) and Mahaim's fibers (nodoventricular tract). The ECG is characterized by (1) very short PR interval (2) P waves are normal , but

the QRS complexes are prolonged and may be aberrant, and there is slurring of the upstroke of the R wave (delta wave).

Table 3: Classification of cardiac arrhythmia. (Bolton, 1975)

Sinoatrial arrhythmias
Sinus arrhythmia
Sinus arrest and sinoatrial block
Wandering pacemaker
Sinus tachycardia
Sinus bradycardia
Ectopic arrhythmia
Supraventricular arrhythmia
Atrial premature beats
Junctional premature beats
Atrial tachycardia
Atrial flutter
Atrial fibrillation
Junctional tachycardia
Ventricular arrhythmias
Ventricular premature beats
Ventricular tachycardia and atrioventricular dissociation
Ventricular fibrillation
Escape rhythms
Junctional escape beats and rhythms
Ventricular escape beats and rhythms
Conduction disturbances
Heart block (AV block)
First degree AV block
Second degree AV block
Third degree AV block
Sinoatrial standstill
Bundle branch block
Right bundle branch block (RBBB)
Left bundle branch block (LBBB)
Wolf-Parkinson-White Sysdrome (WPW)

Mean electrical axis

The mean electrical axis (MEA) refers to the average direction of the electrical potential generated by the heart during the entire cardiac cycle (Tilley, 1985). In veterinary electrocardiography the MEA is usually figured in the frontal plane (Edwards, 1987). The MEA may also be applied to atrial depolarization (P wave) or ventricular repolarization (T wave) but traditionally has been applied to ventricular depolarization (QRS complex) (Tilley, 1988). The MEA in the frontal plane can calculated using the six limb leads and the hexaxial reference system (Figure 11). The net amplitudes in two suitable leads from the hexaxial limb leads are used. Each net of amplitude is plotted on the hexaxial reference system and the perpendicular lines are drawn from these points to their intersection. The line drawn from the center of the axial reference system to the intersection represents the angle (in degrees) of the QRS axis (Figure 12). The normal frontal MEA shows little variation between individual studies. Bone et al. (1988) reported the frontal plane MEA from 25 clinically normal ferrets anesthetized with ketamine-xylazine combination ranging from 79.6-90 degrees (86.13+/-2.5 SD; Bone et al., 1988). The other study reported the MEA ranging from 69 to 97 degree (86+/-6.6 SD) (Smith and Bishop, 1985). The remarkably consistent mean electrical axis of the normal ferret electrocardiogram reflects the long narrow shape of this animal. Unlike cats, which have a normal axis ranging from 0-160 degree (Rogers and Bishop, 1971), or dogs, which have a normal axis ranging from 40 to 100 degrees (Tilley, 1979).

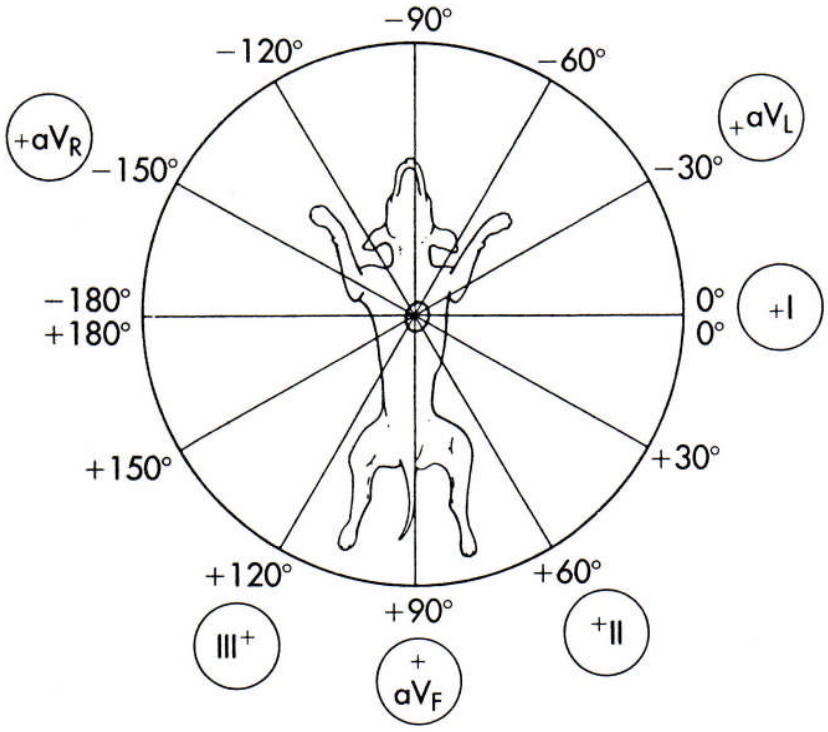

Figure 11: Hexaxial reference system on the frontal plane. The lead axes were marked in 30° increments from 0° to 180°. (Tilley, 1992)

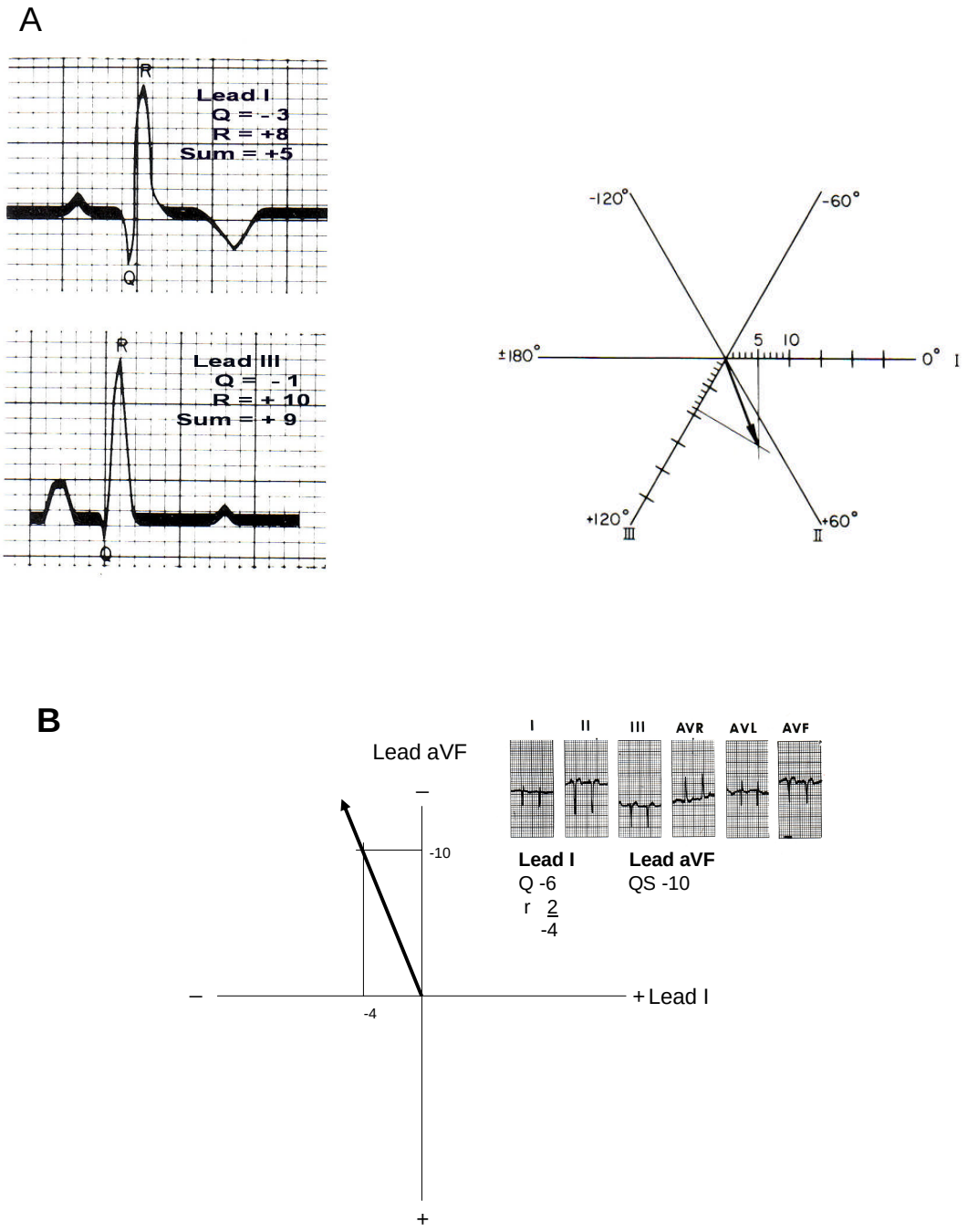

Figure 12: The MEA (frontal vector) in the frontal plane calculated using the six limb leads and the hexaxial reference system. A, Lead I and Lead III were used to demonstrate the calculation method. The net QRS amplitudes from each lead were determined. Each net amplitude was plotted on the hexaxial reference system and the perpendicular lines were drawn from these points to their intersection. The line drawn from the center of the axial reference system to the intersection represents the angle (in degrees) of the axis. B, Lead I and aVF were used to calculate the frontal vector (modified from Trautvetter et al., 1981).

2.2.4. Echocardiography

Basic principles

Ultrasound is a high-frequency sound wave produced by using the electrically stimulated piezoelectric crystal in the transducer. These crystals were deformed (expands and contracts) by electrical voltage and generated the pulsed, high-frequency sound wave (greater than 20,000 Hertz), that is beyond the range of human hearing. The crystals are able to receive sound and convert it back into electrical energy. When the sound waves encounter the difference tissue interface, they are reflected, refracted, absorbed and partially passed into the second tissue interface. Only the reflected waves are sent back to the transducer and produce electrical energy. The echocardiograph computer processes all data to generate an image of the acoustic interfaces on an oscilloscope screen.

Characteristics of sound waves: The sound waves travel in longitudinal lines within the medium with a different speed depending on the density and the stiffness of the medium. The sound travels faster in the high density tissue. For example, the sound travels through the bone at the speed 4080 meter per second (m/sec) and at the speed of 330 m/sec through the air. Acoustic impedance defines the resistance of the flow of sound through a medium. Although increased density increases the speed of sound, the impedance or resistance of sound transmission is high. Since the ability to visualize the structures with ultrasound is determined by the reflection of transmitted sounds, the greater the acoustic mismatch between two adjacent tissues the more reflective and refractive are the boundaries and the stronger are the resulting echos.

Echocardiography (cardiac ultrasound) is the noninvasive method for examination inside the heart including the aorta, the ventricles and atria, the auricular appendages and all the cardiac valves. Three types of echocardiography are used clinically: (1) the two-dimension (2-D) and (2) motion mode (M–mode) echocardiography created by the dynamic images of the contracting heart that provides the tool to evaluate cardiac chamber anatomy and motion while (3) Doppler ultrasound measures the blood flow through the heart and vessels by assessing the relative change in returned ultrasound frequency compared with the transmitted frequency. Cardiovascular defects can be detected, including valvular lesions, cardiac shunts, cardiac and thoracic masses, pleural and pericardial effusions, myocardial disease and stenotic lesions. Echocardiography allows the assessment of cardiac chamber sizes, cardiac function and blood flow, all of which provide information on the hemodynamic status and the extent of a disease process. (Goddard, 1995; Boon, 1998; Ware, 1998; Moise and Fox, 1999)

M-mode echocardiography

M-mode echocardiography was first described as a clinically useful tool in veterinary medicine in 1977 by Pipers and Hamlin (Pipers and Hamlin, 1977). The M-mode images represented the cardiac structure along the axis of the ultrasound beam in a one-dimensional plane. The sharp axial resolution and high sampling frequency of M-mode echocardiography (1000 to 5000 pulses/sec) allow small, rapidly moving structures to be discerned and accurately correlated with time relative to the ECG.

Standard image planes (views) for M-mode echocardiography are derived from 2D images (and mostly from a right parasternal long-axis view of the left ventricle). Standard recordings are made through (1) the aorta and left atrium, (2) left ventricle at the mitral valve level, (3) left ventricle at the level of the chordae tendineae.

The measurements of the aorta and left atrium may be obtained from right parasternal long- or short-axis images. By using the long-axis, the cursor should be placed perpendicular to the walls of the aorta over the valve cusps and through the largest body of the left atrium. From the short-axis view, the cursor should be placed perpendicular to the wall of the aorta through the aortic valve. The aortic root was measured at the end of diastole that coincides with the onset of the QRS complex. If the ECG is not available, one can measure at the lowest point of the aortic wall motion. The left atrium is measured at the largest left atrial chamber size when the aortic walls are at their highest point at end systole (Boon, 2002) (Figure13). The ratio of the left atrium and aortic root size is used to determine the severity of an atrial dilation. In dogs, the left atrial size is similar to the aortic root size. The LA/AO ratio in dogs and cats is usually less than 1.3. Values greater than 1.3 suggest left atrial dilation (Kienle, 1998). Vastenburg et al. (2004) reported the mean LA/AO ratio in ferrets anesthetized with isoflurane is 1.3 with a range between1.0-1.8.

The measurements of the left ventricle can be performed by using the long axis left ventricular out flow view or the short axis view at the level of the chordae tendineae both the systolic and diastolic indices including the septum, the left ventricular chamber and the left ventricular wall are measured. Diastolic measurements are used to assess wall and septal thickness and the systolic measurements are used to assess the function of the left ventricle. The septum is measured from the top of the septal line to the bottom, including the lines that define its boundaries. The left ventriclular chamber is measured from the bottom of the septum to the top of the wall and does not include the lines defining the septal and wall boundaries. The left ventricular wall can be measured from the top of the wall to the top of the pericardial tracing and it includes the line defining the wall and chamber boundary (Boon, 2002) (Figure 14). The left ventricular function can be assessed by using the fractional shortening index (FS). It is calculated by subtracting left ventricular systolic dimension from

the diastolic dimension and divided by the diastolic dimension in order to calculate a percent change in left ventricular size between filling and emptying. The equation is as follows

$$FS = \frac{LVDd - LVDs}{LVDd} \times 100$$

LVDd = left ventricular diastolic dimension

LVDs = left ventricular systolic dimension

M-mode measurements of the mitral valve are made from either the right parasternal long axis or short axis views. They are used to determine the E point to septal separation (EPSS). At slow heart rates, the M-mode of the mitral valve should show an M configuration. The E point on the mitral M-mode represents the rapid ventricular filling phases that occur during early diastole due to atrial blood flow into the ventricle by a pressure gradient. The atrial contraction toward the end of diastole causes the mitral valve to open again and this phase creates the second peak of the M configuration and is referred to as A point. Atrial systolic forces result in about 20% of filling volume in a normal animal that is lesser than the volume of the rapid filling phase. Therefore the A point should be always lower than E point (Boon, 1998; Kienle, 1998; Boon, 2002) (Figure 15). The normal EPSS value in dogs and cats are 0.0-2.0 mm and 0.3-7.7 mm respectively (Boon, 2002). In ferrets, the EPSS value shows a range between 0.0- 2.2 mm (Vastenburg et al., 2004). Patients with moderate to severe DCM show an increase in the EPSS value that is due to decreased blood flow and flow velocity through the mitral valve and an increased cardiac chamber size (Kienle, 1998).

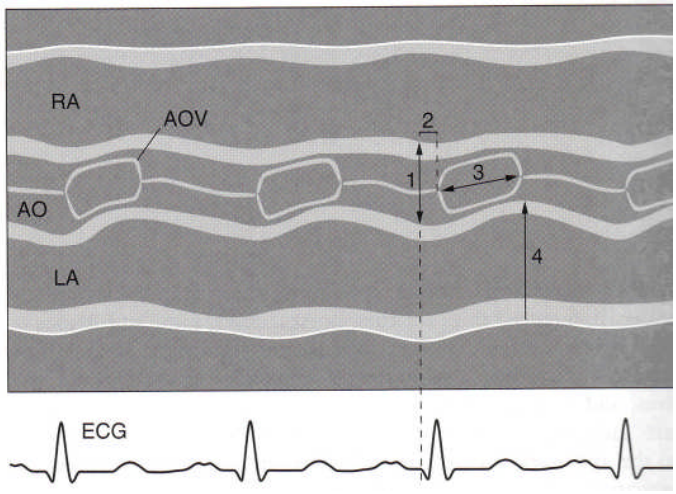

Figure 13: Measurements of the aorta and left atrium. Aortic diameter is measured at the end of diastole that coincides with the onset of the QRS complex. If the ECG is not available, one can measure at the lowest point of the aortic wall motion. The left atrium is measured at the largest left atrial chamber size when the aortic walls are at their highest point at end systole. AO, aorta; RA, right atrium; LA, left atrium; AOV, aortic valve; 1, aortic dimension; 2, pre-ejection period (PEP); 3, left ventricular ejection time (LVET); 4, left atrium dimension. (Boon, 1998)

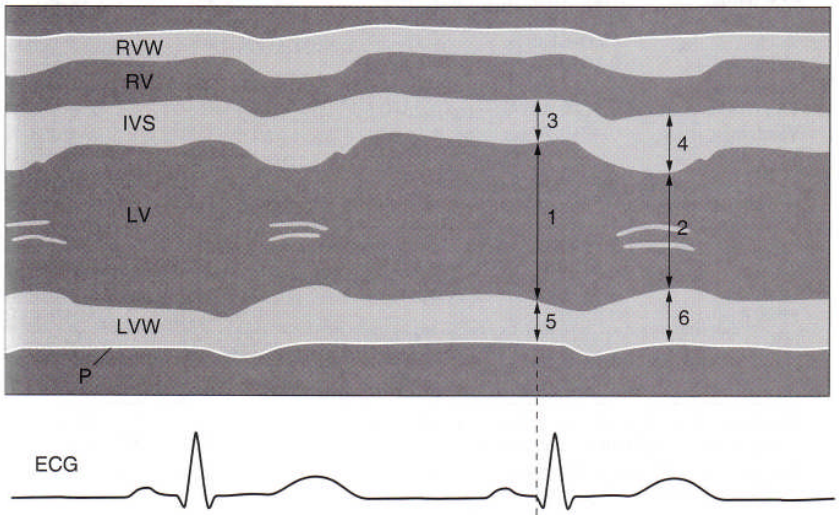

Figure 14: Measurements of the left ventricle: The septum is measured from the top of the septum to the bottom of the septum (3, 4). The left ventricular dimensions are measured from the bottom of the septum to the top of the wall (1, 2). The left ventricular wall is measured from the top of the wall to the top of the pericardial tracing (5, 6). RVW, right ventricular wall; RV, right ventricle; IVS, interventricular septum; LV, left ventricle; LVW, left ventricular wall; P, pericardium; 1, end diastolic dimension; 2, end systolic dimension; 3, septal diastolic thickness; 4, septal systolic thickness; 5, left ventricular wall diastolic thickness; 6, left ventricular wall systolic thickness. (Boon, 1998)

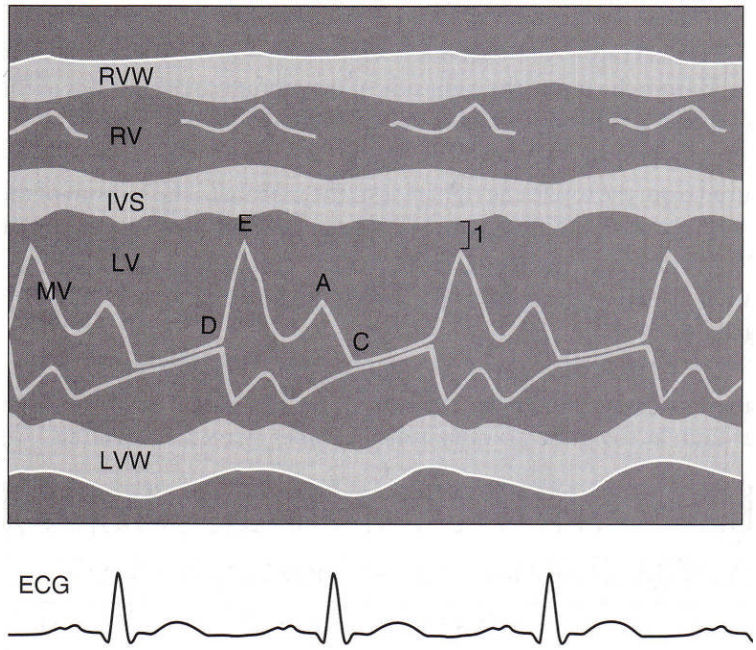

Figure 15: E point to septal separation (EPSS): At a slow heart rate, the M-mode of the mitral valve should show the M configuration. The E point on the mitral M-mode represents the rapid ventricular filling phases and the A point refers to an atrial contraction. RVW, right ventricular wall; RV, right ventricle; IVS, interventricular septum; LV, left ventricle; LVW, left ventricular wall; MV, mitral valve; E, E point; A, A point; 1, EPSS. (Boon, 1998)

Two- dimensional (2-D) echocardiography

Two-dimensional echocardiography was developed to circumvent limitations associated with single beam M-mode interrogations. It creates a fan-shape image, displaying anatomic and functional characteristics that are more anatomically informative than the M-mode image. But the 2-D echocardiography image acuity is less precise, and the frame rate is slower than the M-mode echocardiography. These factors are generally most important when precise measurements of small structures are contemplated. Standard image planes for 2-D echocardiography are designated based upon transducer location (so called windows), special orientation of the imaging plane and the recorded structures.

Right parasternal location: is located between the right 3rd and 6th (usually 4th to 5th) ICS. The two basic imaging planes include the long axis view and the short axis view. The long axis views are generally obtained: (1) a four chamber view and (2) the left ventricular out flow tract, aortic valve and aortic root (Figure 16). The short-axis views provide a series of progressive views at the level of the LV apex, papillary muscles, chordae tendineae, mitral valve and aortic valve (Figure 17). At the long axis view, the subjective assessments are considered normal when the interventricular septum is straight and does not protrude in front of the aorta. The mitral valves are thin and do not prolapse back into the left atrium. The right ventricular chamber is approximately 1/3 of the size of the left ventricular chamber and the right ventricular wall is approximately 1/2 of the thickness of the left ventricular free wall (Boon, 2002). In order to achieve correct accesses in the short axis view one should always view it as a symmetrical circular left ventricular chamber. The papillary muscles are similar in size. The ventricular septum is not flattened and the heart is uniform in contraction. On the level of the heart base, the left atrial size can be measured compared to the aortic root size. The aortic size is measured along the line formed by the commissure of noncoronary and right coronary aortic valve cusps from the inner edge to the inner edge of the aortic wall. The left atrial diameter is measured along the line extending from the commissure of the noncoronary and left coronary aortic valve cusps from the inner edge to the inner edge of the left atrial wall (Oyama, 2004).

Left cranial parasternal location: is located between the left 3rd and 4th ICS between the sternum and costochondral junction. The images obtained from the long and short axis view of the left cranial parasternal location are shown in Figure 18. At this view, the left ventricular out flow tract should be clear of obstruction and the aortic valves are free of lesions. Normally the aorta remains the same diameter all along its length (Boon, 2002).

Left caudal (apical) location: is located close to the sternum between the 5th and 7th ICS. The left apical four- and five-chamber views and the left apical two-chamber views are obtained by this location (Figure 20).

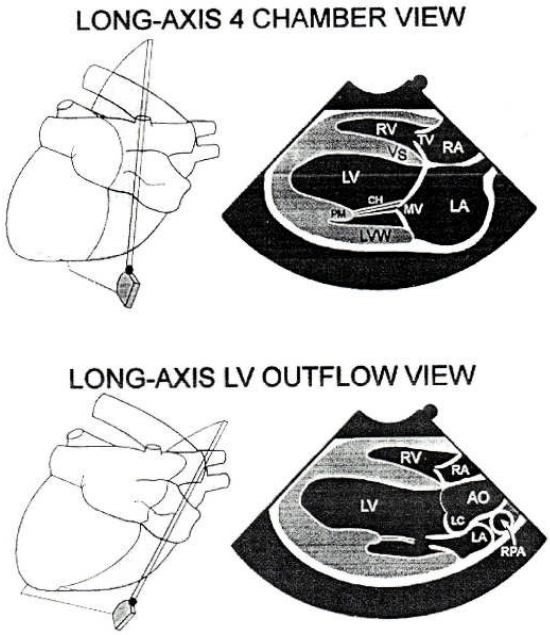

Figure 16: Two-dimensional long axis echocardiogram viewed from right parasternal position. AO, aorta; CH, chordae tendineae; LA, left atrium; LC, left coronary cusp of aortic valve; LV, left ventricle; LVW, left ventricular wall; MA, mitral valve; PM, papillary muscle; RA, right atrium; RPA, right pulmonary artery; RV, right ventricle; TV, tricuspid valve; VS, interventricular septum. (Thomas et al., 1993)

Figure 17: Two-dimensional short axis echocardiographic frames viewed from the right parasternal position. In the center the different positions of the transducer are outlined. A, apex; B, papillary muscle; C, chordae tendineae; D, mitral valve; E, aortic valve; F, pulmonary artery. AO, aorta; AMV, anterior mitral valve cusp; CaVC, caudal vena cava; CH, chordae tendinae; LA, left atrium; LC,RC,NC , left, right ,noncoronary cusps of aortic valve; LPA, left pulmonary artery; LV, left ventricle; LVW, left ventricular wall; MA, mitral valve; PM, papillary muscle; PMV, posterior mitral valve cusp; PPM, posterior papillary muscle; PV, pulmonic valve; RA, right atrium; Rau, right auricle; RPA, right pulmonary artery; RV, right ventricle; RVO, right ventricular outflow tract ; TV, tricuspid valve. (Thomas et al., 1993)

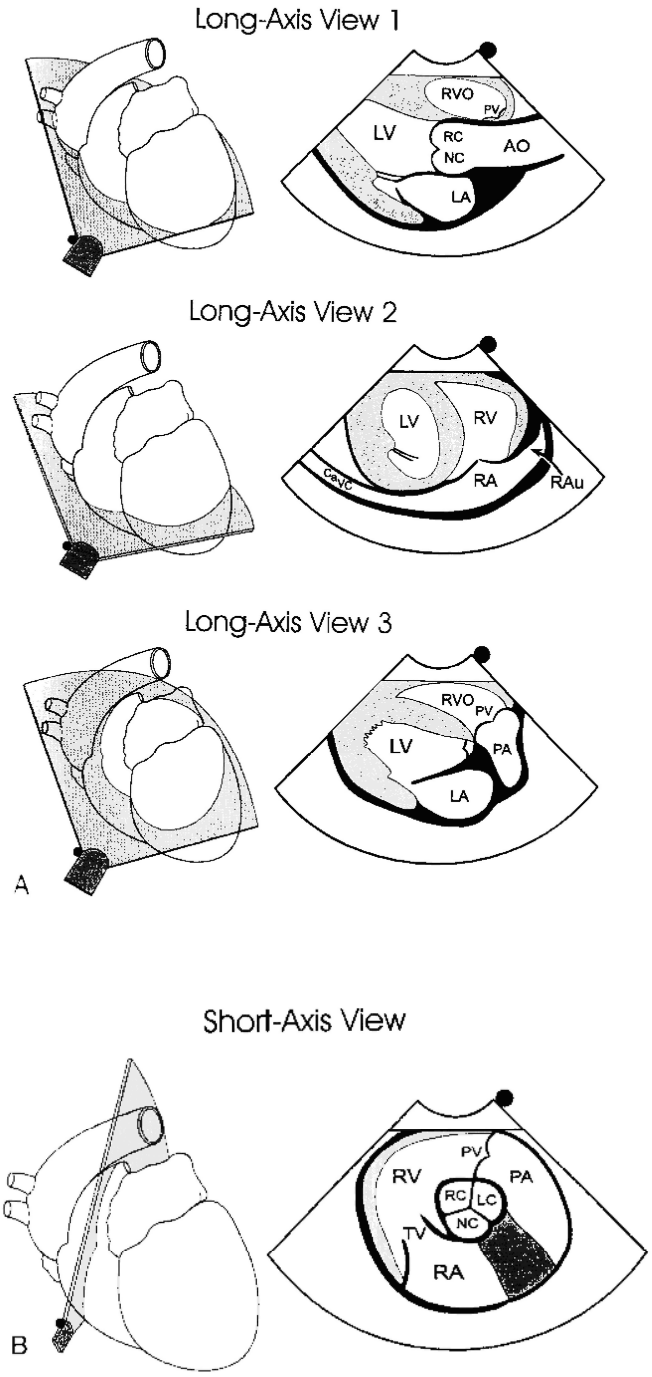

Figure 18: Left cranial parasternal long axis view (A) and left cranial parasternal short axis view (B). LA, left atrium; LC, RC, NC , left, right , noncoronary cusps of aortic valve; LV, left ventricle; PA, pulmonary artery; PV, pulmonic valve; RA, right atrium; Rau, right auricle; RV, right ventricle; RVO; right ventricular outflow tract; TV, tricuspid valve. (Thomas et al., 1993)

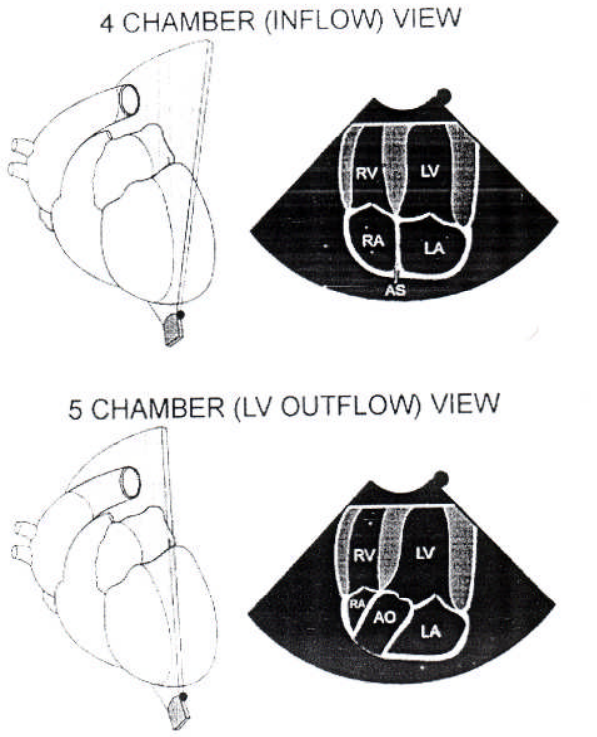

Figure 19: Left caudal (apical) parasternal position. AO, aorta; AS, atrial septum LA, left atrium; LV, left ventricle; RA, right atrium; RV, right ventricle. (Thomas et al., 1993)

Doppler echocardiography (Boon, 1998; Kienle, 1998)

Spectral Doppler: Spectral Doppler echocardiography permits evaluation of the velocity of blood flow and direction within the heart and the great vessels by detection of changes in sound frequency between the emitted ultrasound beam and echos reflected from moving blood cells. Transducer location and imaging planes described for 2-D imaging are used for Doppler echocardiography. The flow across the atrioventricular valve and the aortic flow are performed from the left parasternal position. The flow across the pulmonic valve may be examined from the left or right parasternal position. The maximal flow velocity can be estimated with reasonable accuracy when the angle between the ultrasound beam and blood flow path is less than 20 degrees. Because blood flow patterns and velocity can be evaluated by the Doppler imaging, detection and quantification of valvular insufficiency, valvular stenosis and cardiac shunts are possible (Ware, 1998). The flow velocity can be used to determine the pressure differences between the chambers or vessels by using the modified Bernoulli equation.

$$P1 - P2 = 4 (V2^2 - V1^2)$$

Where, P1 is the pressure proximal to the lesion.
P2 is the pressure distal to the lesion.
V1 is the velocity proximal to the lesion.
V2 is the velocity distal to the lesion.

In small animals, flow velocities in systole in the outflow tract region and great vessels are usually around 1 m/sec. Flow across the AV valves in the diastolic phase shows two waves above the baseline the so called M pattern. The first wave, the E wave that occurs at the early diastolic phase, corresponds to positive filling phase of the ventricle. The second wave, the A wave, is lower than the E wave and occurs in coincidence to the atrial contraction during late diastole (Figure 20). Normally the ratio of the peak E wave to the A wave is greater than one. Peak filling velocities across the AV valve are usually less than 1 m/sec and somewhat less than the velocities across the semilunar valves in the same animal. The flow across the semilunar valve shows a single signal below the baseline (flow away from the transducer). The wave form shows little difference between pulmonic and aortic flow. Flow of the aorta starts just after the end of QRS complex and ends just after the T wave. The aortic flow profile shows an asymmetric appearance. It is composed of a rapid acceleration phase and a deceleration phase. The acceleration phase produces the peak with in the first third of systole. Unlike the aortic flow, the pulmonic peak velocity is reached approximately mid way through the ejection phase that made the flow profile more symmetric and round in appearance. (Figure 21)

Color Flow (CF) Doppler: CF Doppler is a form of pulsed-wave Doppler. Blood flow in color mapping is perceived by the machine as either moving toward or away from the transducer. Flow moving toward the sound source is plotted in hues of red, and flow moving away from the transducer is mapped in shades of blue. The color may range from deep red for slow blood flow to bright yellow for rapid blood flow toward the transducer. Slow blood flow away from the transducer is mapped in deep blue colors, whereas more rapid flow away from the transducer is mapped in shades of light blue and white.

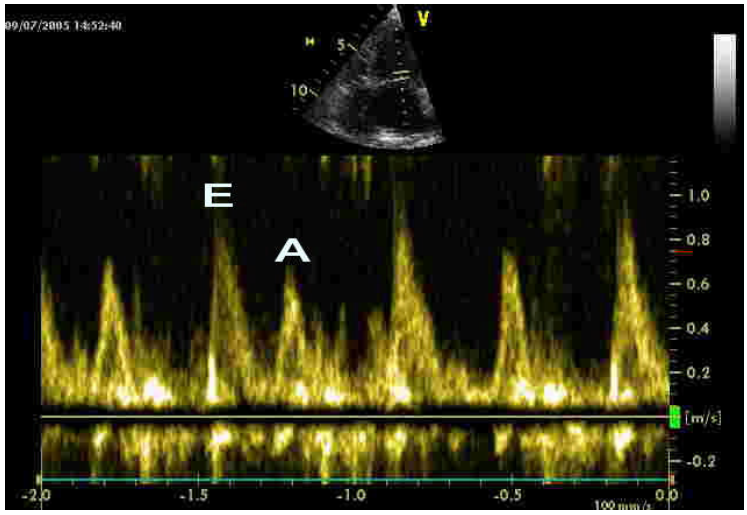

Figure 20: Flow across the AV valve in diastolic phase shows two waves above the baseline. The first wave called E wave occurs at the early diastolic phase, it corresponds to the positive filling phase of the ventricle. The second wave, A wave, is lower than the E wave and coincidences with the atrial contraction during the late diastole.

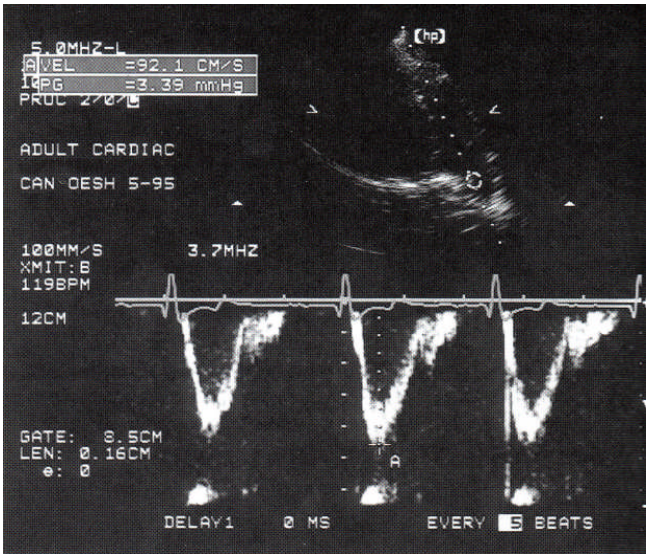

Figure 21: The pulmonic flow starts toward the end of the QRS complex and continued through the T wave. The peak velocity is reached approximately mid way through the ejection producing a symmetric flow profile. (Boon, 1998)

3. Materials and methods

3.1 Materials

All animals were presented to the out patient clinic for cardiovascular examination in the Small Animal Hospital, Free University of Berlin in order to confirm or exclude any type of heart disease. Ninety six ferrets have been enrolled in the special study. All 96 animals underwent a physical examination and a radiographic as well as electrocardiographic examination. Echocardiography was performed in 45 animals that necessitated and tolerated further cardiovascular evaluation.

Thirty one additional cases were collected from the emergency unit for evaluation of dyspnea e.g. using thoracic radiographs. All of these animals were presented to the emergency unit during night, weekend or holiday hours and did not experience a complete cardiologic work up.

3.2 Methods

A routine history was taken from all animals before starting the other clinical examinations. The clinical examinations consisted of auscultation, thoracic radiographic examination, electrocardiographic and echocardiographic examination in additional to observation and palpation.

The patients were classified into 4 subgroups due to the results of clinical examination and anesthetic status as described below.

Group A: non sedated-normal group (NSN group), defined as the patients who underwent a clinical examination without any sedative drugs and had no cardiovascular abnormalities at the time of physical examination.

Group B: non sedated-disease group (NSD group), defined as patients who had a clinical examination without any sedative drugs and were suspected to have cardiovascular abnormalities at the time of presentation (e.g. heart murmur).

Group C: sedated-normal group (SN group), defined as patients who received sedative drugs because they did not tolerate the clinical examinations and eventually no cardiovascular abnormalities were found.

Group D: sedated-disease group (SD group), defined as patients who received sedative drugs because they did not tolerate the complete clinical examinations and were suspected to have cardiovascular abnormalities at the time of presentation.

3.2.1 Anesthetic procedures

Ketamine hydrochloride (5-8 mg/kg) combination with xylazine (0.5 mg/kg) was given intramuscularly to anesthetize the animals whenever necessary.

3.2.2 Auscultation procedures

All patients were auscultated on the both sides of the chest wall. The cardiac auscultation was performed over the mitral valve, pulmonic valve and the aortic valve area between the 6^{th} to 8^{th} intercostal spaces on the left chest wall (Stamoulis et al., 1997; Ivey and Morrisey, 1999). For the tricuspid valve region, the stethoscope was placed on the right side of the chest over the PMI of the tricuspid valve. A Littmann classic II stethoscope (3M Company, USA) or Rapaport-Sprague stethoscope (Hewlett-Packard, USA) was used. During auscultation, heart sounds, heart rhythm, and heart rate were assessed. The intensity of the murmurs was scored in I to V grades (Detweiler and Patterson, 1967):

Grade I:	The softest audible murmur.
Grade II:	A faint murmur, clearly heard after a few seconds auscultation.
Grade III:	Immediately heard when auscultation begins and audible over a fairly large area.
Grade IV:	The loudest murmur which is still inaudible when the stethoscope chest piece is just removed from the thoracic wall.
Grade V:	A murmur that remains audible when the stethoscope chest piece is removed from the thoracic wall.

3.2.3 Electrocardiographic examination

Animal positioning and restraint

Each ferret was positioned in right lateral recumbency for the electrocardiographic examination. The animal's limbs were positioned perpendicular to the long axis of the body and parallel to each other.

Attaching the leads

The alligator clip electrodes were attached to the appropriate arm just below the elbow, and the leg leads were attached to the appropriate leg just above the stifle. The skin at the contact site was saturated with alcohol and/or electrode gel to establish good electrode contact and prevent electrical interference.

Registration

All electrocardiograms were recorded at a paper speed of 25 and/or 50 mm/sec and the machine (EK53, PPG HELLIGE GmbH, Freiburg) was standardized at 1 cm = 1 mV or 0.5 cm = 1 mV.

Lead system

Bailey's hexaxial lead system (bipolar limb leads and augmented unipolar limb leads) was used in this study. In the bipolar limb leads, the electrodes are attached to the right forelimb (RA), the left forelimb (LA), and the left hindlimb (LL). The right hindlimb (RL) connects the patient to the ground electrode. In lead I, the RA is the negative terminal and LA is the positive terminal. In lead II, RA is the negative terminal and LL is the positive terminal. In lead III, LA is the negative terminal and LL is the positive terminal. More details of the augmented unipolar limb leads see Table 1, page 17.

Evaluation

The HR, heart rhythm, MEA or frontal vector, duration and amplitude of the ECG waves and the ECG abnormalities were evaluated. The HR was calculated by counting the number of the complexes that occur in 3 seconds (30 boxes) at a paper speed 50 mm/sec and multiplied by 20. At the paper speed of 25 mm/sec, the HR was calculated by counting the number of the complexes that occur in 6 seconds (30 boxes) and multiplied by 10 (Figure 22). The amplitude and duration of the P wave, PR interval, R wave amplitude, QRS interval, PQ duration, S wave amplitude, T wave amplitude, QT duration and heart rate were determined always from lead II. (See Figure 8, page 16)

Figure 22: Paper speed 25 mm/sec, the heart rate can be calculated by counting the number of the QRS complexes in 6 seconds (30 boxes, from 0 sec to 6th sec) and multiplied by 10. On this tracing, the HR is 250 bpm (25x10). Paper speed 25 mm/sec, sensitivity 1 cm/mV.

Determination of the mean electrical axis (MEA) or frontal vector

The frontal QRS vector was contributed from the ECG of 25 ferrets from the normal groups (group A, NSN and group C, SN) and 26 ferrets from the disease groups (group B, NSD and group D, SD). The MEA was determined by examining the QRS complexes in lead I and aVF by the following steps (See Figure 12):

1. Determine the net deflection of the QRS complex in lead I and aVF.
2. The net deflection value was plotted on each lead in reference chart (Bailey's hexaxial lead system) and a perpendicular line was drawn from each lead.
3. A line drawn from the center of the axis chart to the point at which the two perpendicular lines meet and the angle was determined.

3.2.4 Radiographic examination

Radiographic techniques

The lateral and dorsoventral thoracic radiographs were taken in all animals. Mammography films were used with calciumwolframat amplification foils. All radiographs were made with a technique of 49-55 kVp and 3 mAs at a focus-film distance of 36 inches.

In selected cases, angiocardiograms were performed in order to differentiate from possible congenital lesions or demonstrate the proportions of the whole heart and the cardiac structures in comparison to the thoracic cavity. A nonselective technique with cannulas or catheters in a peripheral vein was preferred in order to avoid anesthesia. A 70% iodine salt contrast medium (0.8 ml/kg) was used for all angiocardiograms.

Determination of cardiac size by using the conventional intercostal space score and the heart/thorax ratio. (Kealy, 1991)

At first all chest X-rays were judged subjectively using the conventional intercostal space score procedures. The heart size was determined regarding to the number of intercostal spaces on the lateral position.

The heart/thoracic ratio was calculated by using the radiograph positioned laterally. The height of the heart was measured from the heart apex to the base (L) and the height of the thoracic cavity was measured from the upper to the lower thoracic wall through heart base and apex (T) (Figure 23).

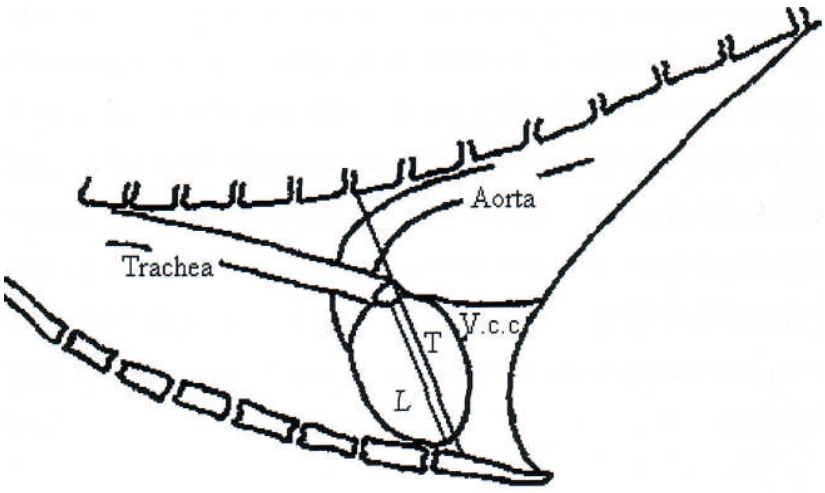

Figure 23: The heart/thoracic ratio. L, maximum height of the heart; T, maximum height of the thorax; V.c.c, caudal vena cava. (Kirchhoff, 2003)

Determination of cardiac size by using a modified vertebral heart score. (Stepien et al., 1999)

In the lateral view, the long axis of the heart (L) was measured with a caliper extending from the bottom of the left mainstem bronchus to the apex of the heart. The caliper was repositioned along the vertebral column, starting at the cranial edge of the fifth thoracic vertebra. The length of the heart was registered as the number of vertebrae and estimated to the nearest 1/4 of a vertebra. The short axis (S) was measured perpendicular to the long axis at the level of the caudal vena cava. The length of S was recorded in the same manner beginning at the fifth thoracic vertebra. The vertebral heart sum (VHS) was determined by the sum of the long and the short axis (Figure 24). On the DV view, the long axis of the heart was measured from midline of the cranial edge of the cardiac silhouette to the apex. The short axis was measured in the middle third perpendicular to the long axis. The length of the long and the short axes were compared to the vertebral length on the DV view, beginning at the cranial edge of the fifth thoracic vertebra. The VHS of the DV view is equal to the sum of the long and the short axis (Figure 25).

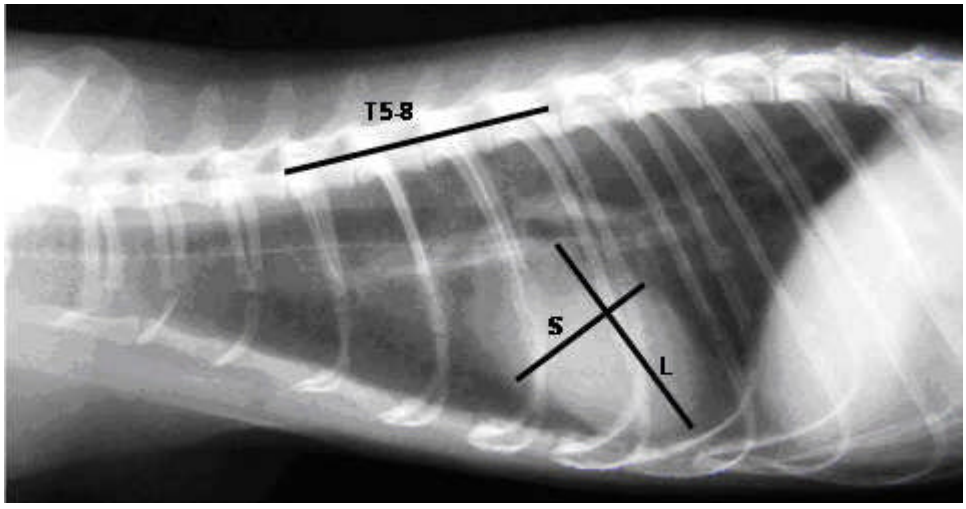

Figure 24: On the lateral view, the long axis of the heart (L) is measured from the bottom of mainstem bronchus to the apex of the heart. The short axis (S) is measured perpendicular to the long axis at the level of caudal vena cava. The length of the heart is recorded as the number of vertebrae which starts at the cranial edge of the fifth thoracic vertebra. Long plus short axis = VHS.

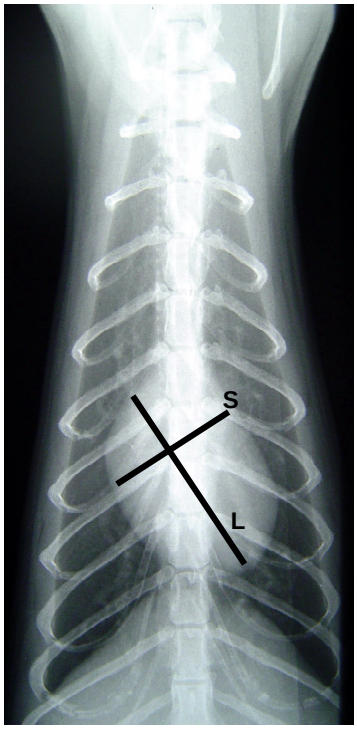

Figure 25: On the DV view, the long axis of the heart is measured from the midline of the cranial edge of the cardiac silhouette to the apex. The short axis is measured in the middle third perpendicular to the long axis. The length of the long and short axis is given by the number of vertebrae in the DV position. (See Figure 23)

Examination of the lung fields, lung vessels and the trachea

The lung fields and lung vessels were examined on the lateral and dorsoventral views. The lung fields, the lung vessels and abnormalities such as e.g. pleural effusion and tumors were also evaluated. The abnormality patterns of the lung fields were assessed as described by Kealy (1999).

(1) Alveolar pattern
(2) Interstitial pattern
(3) Bronchial pattern

The angle between the trachea and the thoracic vertebrae was evaluated. It was classified into three groups depending on the degree of an angle (1) 0 degree or trachea parallel to the thoracic vertebrae, (2) any angle between 1-10 degrees, and (3) an angle of more than 10 degrees.

The lung vessels were examined on the lateral view by scrutinizing the size of the pulmonary vein and artery in the cranial lobe.

Dyspneic cases not included in the cardiovascular group.

Thirty one animals with dyspnea were added to this study. All 31 ferrets were presented with more or less severe dyspnea and radiographs were taken in order to make a tentative diagnosis. These animals were brought to the clinic predominantly during night, weekend or holiday hours. In this group clinical infectious-inflammatory signs as well as corresponding radiographic changes on the thoracic films were observed mainly. No detailed cardiovascular examination could be performed for different reasons.

3.2.5 Echocardiographic examination

Forty five animals were enrolled for echocardiographic examinations. All examinations were performed by using a Sigma 44 HVCD model machine (Sigma 44 HVCD model, Kontron Instrument Company) with a 7.5 MHz mechanical probe. The data were recorded using a trackball-driven cursor and ultrasound system software. At first, in each animal the hair was clipped on the thoracic wall, caudal to the scapular level, where the ictus cordis was palpated. The animals were placed on right lateral recumbency over the gap on the ultrasound table. ECG was recorded on each animal by placing the alligator clip electrodes just below to the left and right olecranon and proximal to the stifle. The M-mode, 2-D and Doppler (in selected cases) echocardiography was used to evaluate size, structures, function and hemodynamic status of the heart.

Measurements of the left ventricle

The measurement of the left ventricle was performed on the right lateral position. The short and/or long axis 2-D image of the left side was used for an M-mode to measure the LV. The systolic and diastolic thickness of left ventricular free wall (LVW), interventricular septum (IVS) and left ventricular internal diameter (LVID) were measured. Diastolic measurements were made at the onset of the QRS complex of a simultaneously recorded ECG. Systolic measurements of the left ventricle were made from the point of peak downward motion of the septum to the leading edge of the left ventricular free wall endocardium. The septum was measured from the top of the septum to the bottom of the septum, including the lines that define its boundaries. The left ventricular chamber was measured from the bottom of the septum to the top of the wall, excluding the lines of the septal and wall boundaries. The left ventricular wall was measured from the top of the wall to the top of the pericardial sac, including the line of the wall and the chamber boundary. (See Figure 14, page 29)

Evaluation of the systolic function

The FS was used to determine the left ventricular function. FS was calculated automatically by subtracting left ventricular systolic dimension from the diastolic dimension divided by the diastolic dimension to calculate a percental change in left ventricular size. The equation is as follows:

$$FS = \frac{LVDd - LVDs}{LVDd} \times 100$$

LVDd = left ventricular diastolic dimension
LVDs = left ventricular systolic dimension

Evaluation of the aorta and left atrial size

The images were obtained from the right parasternal position. For the long-axis left ventricular out flow view, the measurement was performed by placing the cursor perpendicular to the walls of the aorta over the aortic valves cusps and through the largest body of the left atrium. An M-mode image of this plane was recorded. The aorta was measured from the onset of the QRS complex, at the lowest point of aortic wall motion. The measurement was performed from the top of the anterior aortic wall to the top of the posterior aortic wall at end diastole. The measurement of the left atrium was made at the largest left atrial size when the aortic walls were at the highest points. The left atrium was measured from the top line of the posterior aortic wall to the top of the pericardium. The left atrium to aortic root size ratio was calculated. (See Figure 13, page 28)

Spectral Doppler examination

In the selected cases, the blood flow velocities and patterns across the heart valves were determined by using spectral Doppler echocardiography.

Aortic flow: The left apical five chamber view was used to determine the flow across the aortic valves (Figure 19, page 33). The Doppler gate was positioned just distal to the aortic valve.

Pulmonic flow: The pulmonic flow was recorded from the right parasternal view of the left ventricle with the pulmonary artery view or the left parasternal short axis plane with aorta and pulmonary artery or the left parasternal long axis with right ventricular outflow view (Figure 18, page 32). The Doppler gate is placed distal to the valve within the pulmonary artery.

Mitral flow: The mitral flow was recorded from the left parasternal apical four or five chamber planes (Figure 19). The Doppler gate is placed at the tip of the leaflets when the valves are wide open.

3.3 Statistical analysis

SPSS version 10.0 was used for analyzing the data. The descriptive analysis was used to determine the maximum, minimum, mean, median and standard deviation of the data.